

Lecture Book Drive Systems

D. T. McGuiness, PhD

Version: 2025.SS

Contents

I. DC Machines	3
1. Modelling DC Machines	5
1.1. Introduction	5
1.2. Operation Principle	6
1.3. Induced EMF	7
1.4. Equivalent Circuit and Electromagnetic Torque	9
1.5. Electromechanical Modelling	10
1.6. State-Space Modelling	10
1.7. Block Diagrams and Transfer Functions	11
1.8. Field Excitation	12
1.8.1. Separately Excited	12
1.8.2. Shunt Excited	14
1.8.3. Series Excited	14
1.8.4. Compound	15
1.8.5. Permanent-Magnets	15
1.9. Measuring the Motor Constants	16
1.9.1. Armature Resistance	16
1.9.2. Armature Inductance	16
1.9.3. EMF Constant	17
1.10. Simulation	17
1.10.1. Separately-Excited	17
II. Induction Machines	21
2. Induction Motor Dynamics and Control	23
2.1. Introduction	23
2.2. Steady-State Analysis	24
2.2.1. Speed of Operation	24
2.2.2. Normal Operation	26
2.3. Construction	27
2.4. Dynamic Modelling	33
2.4.1. Real Time Model of a Two-Phase Induction Machine	34
2.4.2. Transformations for Constant Matrices	36
2.4.3. Three-Phase to Two-Phase Transformation	39

2.4.4.	Power Equivalence	42
2.4.5.	Generalised Model in Arbitrary Reference Frame	42
2.4.6.	Electromagnetic Torque	44
2.4.7.	Derivation of Commonly Used Induction-Machine Models	46
2.4.8.	Equations in Flux Linkages	49
2.5.	Dynamic Simulation Equations	50
2.5.1.	Simulation Example	52
2.5.2.	No-load Startup	53
2.5.3.	Application of a Step Torque Load	55
Bibliography		61

List of Figures

1.2. A close-up view of the Direct Current (DC) machine. Please observe the commutator part of the motor (left size and the brushes which are a signature feature of these kind of machines [8].	6
1.1. A pair of carbon brushes used in DC drives which allow commutation. While solid-state commutation has become popular in the last decades, their cost effective nature still makes them the prevalent choice in industry [7].	6
1.3. A Schematic representation of a DC machine during operation with the path of the flux lines shown.	7
1.4. Equivalent circuit of a DC machine.	9
1.5. Block diagram of a DC motor.	11
1.6. Circuit diagram of a separately-excited DC machine.	12
1.7. Circuit diagram of a separately-excited DC machine.	14
1.8. Circuit diagram of a separately-excited DC machine.	14
1.9. Circuit diagram of a separately-excited DC machine.	15
1.10. Induced Electro-motive Force (EMF) v. rotor speed characteristics at rated field current.	17
1.11. The simulation diagram of a separately excited DC machine.	17
1.12. Simulation Results of the separately-excited DC motor.	18
2.1. Cross-sectional view of Induction Machine (IM) [13].	23
2.2. A wound-rotor IM [20].	24
2.3. Steady-state torque behaviour of an IM. Here important parameters and concepts can be observed. An important aspect is to mention is the stability of an IM only occurs between %2 to %8 slip during normal operation.	26
2.4. Lamination on a stator is done to reduce eddy currents [13].	27
2.5. Form winding.	30
2.6. The materials used in the construction of an IM.	33
2.7. Stator and rotor winding of a two-phase IM. The model shows the stator inductances as L_{qs} and L_{ds} , and the rotor as L_{α} and L_{β} . as the rotor spins these inductances will interact with one another and produce mutual inductance.	34
2.8. Transformation on actual to fictitious rotor variables.	37
2.9. A Simulink Model of an Induction Machine.	53
2.10. The parametric plot of rotor speed v. torque when the motor starts from standstill without an external load.	54
2.11. The parametric plot of rotor speed v. torque when an instantenous load is applied to the motor at 0.4 s.	54

2.12. Simulation results for starting IM from standstill.	56
2.13. Simulation of the IM when an instantenous load is applied to the motor at 0.4 s. .	57

List of Tables

1.1. Simulation parameters for the separately-excited DC motor.	18
2.1. Simulation parameters for the IM example.	52

Part I.

DC Machines

Chapter 1

Modelling DC Machines

Table of Contents

1.1. Introduction	5
1.2. Operation Principle	6
1.3. Induced EMF	7
1.4. Equivalent Circuit and Electromagnetic Torque	9
1.5. Electromechanical Modelling	10
1.6. State-Space Modelling	10
1.7. Block Diagrams and Transfer Functions	11
1.8. Field Excitation	12
1.9. Measuring the Motor Constants	16
1.10. Simulation	17

1.1. Introduction

DC machines have been in service for more than a century [1]. Their structure has changed a great deal since the introduction of the IM¹. DC machines have seen a resurgence of use with the advent and cost effective nature of the Silicon Controlled Rectifier (SCR) [2], facilitating a wide-range speed control of these motors and are still used in a wide range of industries such as mining [3], automotive industries [4], and public transportation [5].

¹Due to historical reasons, IM is also called Alternating Current (AC) shunt motor by people who refuse to keep up with the times.

A great benefit of DC machines over any type is its simple control mechanisms.

This chapter contains a brief description of the theory of operation of separately-excited² and Permanent Magnet (PM) DC brush motors and of their modeling and transfer functions, an evaluation of steady state and transient responses. A representation of the motor can be seen in Fig. 1.2.

²One of the more industrially relevant DC motor connection.

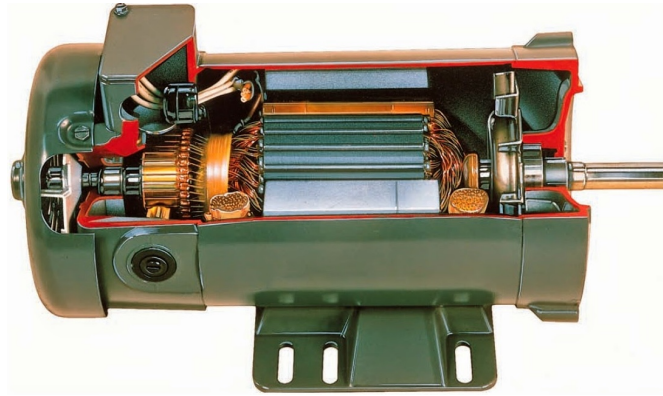


Figure 1.2.: A close-up view of the DC machine. Please observe the commutator part of the motor (left side) and the brushes which are a signature feature of these kind of machines [8].

1.2. Operation Principle

³Recall that a wire in an external field experiences maximum torque when the field passes the wire perpendicularly.

It is well known that maximum torque is produced when two (2) fluxes are in quadrature³ [6]. The fluxes are created with two (2) current-carrying conductors. The flux path is of low reluctance with steel. **Fig. 1.2** shows such a schematic representation.

Coil 1: Field Winding wound on the pole produces a flux (ϕ_f) with an input current i_f .

Coil 2: Armature Winding called the armature winding on a rotating surface produces a flux ϕ_a with a current i_a .

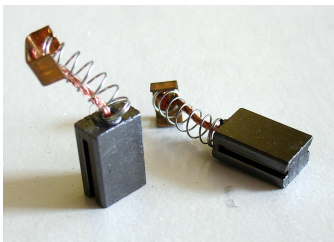


Figure 1.1.: A pair of carbon brushes used in DC drives which allow commutation. While solid-state commutation has become popular in the last decades, their cost effective nature still makes them the prevalent choice in industry [7].

⁴i.e., unidirectional torque.

For the given position, the two (2) fluxes are mutually perpendicular ($\phi_f \perp \phi_a$) and will in turn exert a maximum torque on the rotor. This in turn will move the rotor in **clockwise** direction. If we assume the rotor has moved by 180° , coils which were under the influence of south pole will be under the south pole and will be carrying negative current.

The generated torque will be such as to move the rotor in the **counterclockwise** direction, keeping the rotor in oscillation. To have a uniform torque⁴ and a clockwise (or counterclockwise) direction of rotation, the armature winding needs to carry a current of the same polarity underneath a field pole. That is arranged by separating the armature coils and connecting them to separate copper bars, called a **commutator**, mounted on the same shaft as the armature and field from tubes.

The brushes are stationary and supplied with currents of fixed polarity. This means the commutator segments under a brush will continue to receive a current of fixed polarity. [9]

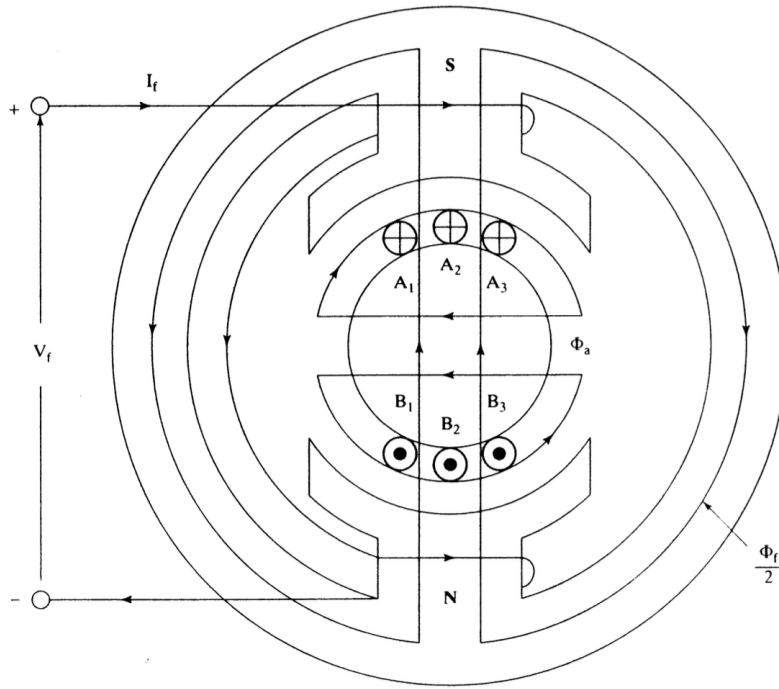


Figure 1.3.: A Schematic representation of a DC machine during operation with the path of the flux lines shown.

1.3. Induced EMF

The mathematical expression for induced emf (e) and torque is derived for a machine with P poles, Z armature conductors in a field with a flux per pole of ϕ_f and its rotor rotating at n_r rpm.

According to Faraday's law⁵, the induced EMF (neglecting the sign) is:

$$e = Z \frac{d\phi_f}{dt} = Z \frac{\phi_f}{t} \quad (1.1)$$

where t is the time taken by the conductors to cut ϕ_f flux lines. Therefore:

$$t = \frac{1}{2 \times \text{frequency}} = \frac{1}{2 \left(\frac{P}{2} \right) \left(\frac{n_r}{60} \right)} \quad (1.2)$$

The flux change occurs for each pole pair. By substituting Eq. (1.1) in Eq. (1.2):

$$e = \frac{Z \phi_f P n_r}{60}$$

If the armature conductors are divided into a parallel paths⁶, then:

$$e = \frac{Z \phi_f P n_r}{60a} \quad (1.3)$$

⁵For a brief refreshment, please look at the lecture materials for M.Sc Electrodynamics

⁶How a motor is wound is paramount during design as some windings can improve efficiency, decrease torque pulsations or determine parameters such as speed. However this topic is too detailed for this margin to contain and beyond the scope of this lecture.

There are two (2) possible arrangements of conductors in the armature, wave windings and lap windings. The values of a for these two (2) types of windings are:

$$a = \begin{cases} 2 & \text{for wave winding} \\ P & \text{for lap winding} \end{cases}$$

It is usual to write the expression Eq. (1.3) in a **compact** form as:

$$e = K\phi_f\omega_m,$$

where $\omega_m = 2\pi n_r/60 \text{ rad s}^{-1}$, and

$$K = \left(\frac{P}{a}\right) Z \left(\frac{1}{2\pi}\right).$$

In literature K is defined as a **machine constant**. The name comes from the fact all parameters making up the constant are defined during the construction of the machine and therefore are fixed values during operation. If the field flux is assumed to be **constant**, then the **induced emf is proportional to the rotor speed** and the constant of proportionality is known as the **induced emf**⁷ or constant. Then the induced emf is represented as:

⁷also known as back emf

$$e = K_b\omega_m, \quad (1.4)$$

where K_b is the induced emf constant, given by the relation:

$$K_b = K\phi_f \text{ V rad}^{-1} \text{ s}^{-1}$$

The field flux (ϕ_f) is written as the ratio between the field Magneto-motive Force (MMF) and mutual reluctance \mathcal{R}_m ,

$$\phi_f = \frac{N_f i_f}{\mathcal{R}_m}, \quad (1.5)$$

where N_f is the number of turns in the field winding, i_f is the field current, and \mathcal{R}_m is the reluctance of the mutual flux path⁸.

⁸This topic was covered in **B.Sc Drive Technologies** where, if need be, all materials are in its respective GitHub repo.

The mutual flux is the resultant of the armature and field fluxes.

By substituting Eq. (1.5) into Eq. (1.4), the emf constant is obtained as:

$$K_b = \frac{KN_f i_f}{\mathcal{R}_m} = M i_f \quad (1.6)$$

where M is the **fictitious mutual inductance** between armature and field windings given by:

$$M = \frac{KN_f}{\mathcal{R}_m} = \left(\frac{P}{\pi}\right) \frac{Z}{2a} \frac{N_f}{\mathcal{R}_m}$$

Here $Z/(2a)$ is the number of turns in the armature per parallel path and together in product with the field winding turns N_f gives the familiar mutual inductance definition.

The factor P/π makes it a **fictitious inductance**.

By substituting Eq. (1.6) to Eq. (1.4), the induced emf is obtained as:

$$e = M i_f \omega_m \quad (1.7)$$

The mutual inductance is a function of the field current and must be taken note of to account for saturation of the magnetic material⁹. For operation within the linear range, mutual inductance is assumed to be a constant in the machine.

⁹i.e., effects caused by stator laminations.

1.4. Equivalent Circuit and Electromagnetic Torque

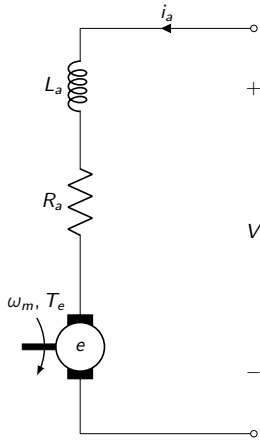


Figure 1.4.: Equivalent circuit of a DC machine.

The equivalent circuit of a DC motor armature¹⁰ is based on the fact that the armature winding has a resistance R_a , a self-inductance L_a , and an induced emf.

This is shown in **Fig. 1.4**. In the case of a motor operation, the input is electrical energy and the output is the mechanical energy, with an air gap torque of T_e at a rotational speed of ω_m . The terminal relationship is written as

$$v = e + R_a i_a + L_a \frac{di_a}{dt} \quad (1.8)$$

In steady state, the armature current is constant and hence the rate of change of the armature current is zero. Hence the armature equation reduces to

$$v = e + R_a i_a \quad (\text{Steady-state}) \quad (1.9)$$

The power balance is obtained by multiplying Eq. (1.9) by i_a :

$$v i_a = e i_a + R_a i_a^2$$

The term $R_a i_a^2$ denotes the armature copper losses and $v i_a$ is the total input power. Therefore, $e i_a$ denotes the effective power that has been transformed from electrical to mechanical form, which we will call the air-gap power (P_{ag}).

The air-gap power¹¹ is expressed in terms of the electromagnetic torque (T_e) and rotor speed (ω_m) as:

$$P_{ag} = \omega_m T_e = e i_a$$

This allows us to represent the electromagnetic torque or air gap torque as:

$$T_e = \frac{e i_a}{\omega_m} \quad (1.10)$$

¹⁰Armature is a term that is often confused and here in this side margin I hope to clarify a bit.

Technically, armature is the part of the machine which has AC current flowing in. Therefore in a DC machine it is the rotor but for a AC machine this could be the stator. This term is mostly an old term and is mostly used in describing DC machine construction.

¹¹Air gap power can be defined as the transferred power from the stator to the rotor.

By substituting for the induced EMF from Eq. (1.4) into Eq. (1.10), it is further simplified to be:

$$T_e = K_b i_a \quad (1.11)$$

The torque constant (K_b) is equal to the EMF constant if it is expressed in volt-sec/rad for a constant-flux machine.

1.5. Electromechanical Modelling

To keep thing simple, the load is modeled as a moment of inertia (J) in $\text{kg m}^2 \text{s}^{-2}$, with a viscous friction coefficient¹² B_l in N. Then the acceleration torque (T_a) given in N m drives the load and is given by:

$$J \frac{d\omega_m}{dt} = B_l \omega_m = T_e - T_l = T_a \quad (1.12)$$

where T_l is the load torque. Eq. (1.8) and Eq. (1.12) constitute the dynamic model of the DC motor with load.

1.6. State-Space Modelling

The dynamic equations can be written in state-space form and are given by:

$$\begin{bmatrix} p_t i_a \\ p_t \omega_m \end{bmatrix} = \begin{bmatrix} -\frac{R_a}{L_a} & -\frac{K_b}{L_a} \\ -\frac{K_b}{J} & -\frac{B_l}{J} \end{bmatrix} \begin{bmatrix} i_a \\ \omega_m \end{bmatrix} + \begin{bmatrix} \frac{1}{L_a} & 0 \\ 0 & -\frac{1}{J} \end{bmatrix} \begin{bmatrix} V \\ T_l \end{bmatrix} \quad (1.13)$$

where p_t is the differential operator with respect to time. Eq. (1.12) is expressed compactly in the form given by

$$\dot{\vec{X}} = \vec{A}\vec{X} + \vec{B}\vec{U}$$

where:

$$\vec{X} = [i_a \quad \omega_m]^T, \quad \text{and} \quad \vec{U} = [V \quad T_l]^T.$$

Here \vec{X} is the state variable vector, and \vec{U} is the input vector. Even though the load torque is a disturbance, for sake of a compact representation it is included in the input vector in this text.

$$\vec{A} = \begin{bmatrix} -\frac{R_a}{L_a} & -\frac{K_b}{L_a} \\ -\frac{K_b}{J} & -\frac{B_l}{J} \end{bmatrix}, \quad \vec{B} = \begin{bmatrix} \frac{1}{L_a} & 0 \\ 0 & -\frac{1}{J} \end{bmatrix}$$

The roots of the system are evaluated from the A matrix, which are:

¹²This basically means the load is working with liquids which are resistant to moving. Cement mixing would be a good example.

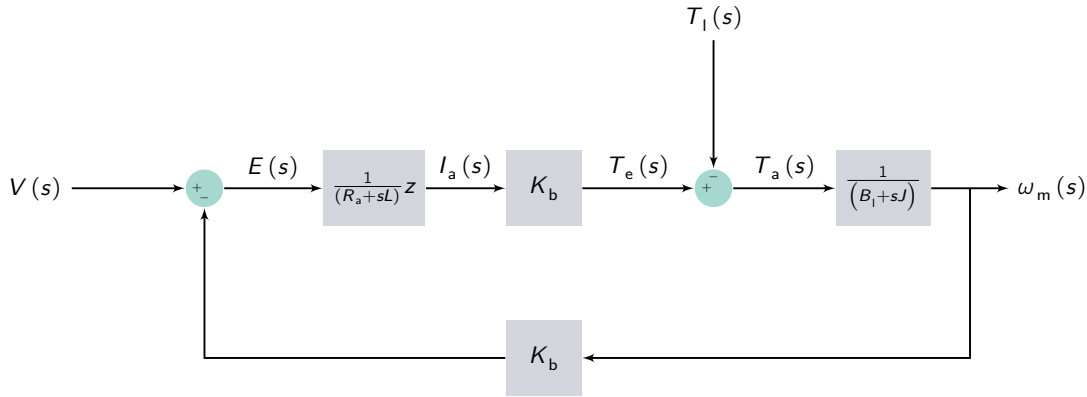


Figure 1.5.: Block diagram of a DC motor.

$$\lambda_{1,2} = \frac{-\left(\frac{R_a}{L_a} + \frac{B_l}{J}\right) \pm \sqrt{\left(\frac{R_a}{L_a} + \frac{B_l}{J}\right)^2 - 4\left(\frac{R_a B_l}{J L_a} + \frac{K_b^2}{J L_a}\right)}}{2} \quad (1.14)$$

It is interesting to observe that these eigenvalues will **always have a negative real part**.

This indicates the the motor is stable on open-loop operation.

1.7. Block Diagrams and Transfer Functions

Taking Laplace transforms of Eq. (1.8), Eq. (1.12) and neglecting initial conditions, we get

$$I_a(s) = \frac{V(s) - K_b \omega_m(s)}{R_a + sL_a} \quad \text{and} \quad \omega_m(s) = \frac{K_b I_a(s) - T_l(s)}{B_l + sJ} \quad (1.15)$$

The relationship is represented in **Fig. 1.5**. We derive the transfer functions as follows:

$$G_{\omega V}(s) = \frac{\omega_m(s)}{V(s)} = \frac{K_b}{s^2 (JL_a) + s (B_l L_a + J R_a) + (B_l R_a + K_b^2)} \quad (1.16)$$

$$G_{\omega I}(s) = \frac{\omega_m(s)}{T_l(s)} = \frac{-(R_a + sL_a)}{s^2 (JL_a) + s (B_l L_a + J R_a) + (B_l R_a + K_b^2)} \quad (1.17)$$

The separately-excited DC motor is a **linear system**, and therefore the speed response due to the simultaneous voltage input and load torque disturbance can be written as a **sum of their individual responses**:

$$\omega_m(s) = G_{\omega V}(s)V(s) + G_{\omega I}(s)T_l(s) \quad (1.18)$$

Laplace inverse of $\omega_m(s)$ in Eq. (1.18) gives the time response of the speed for a simultaneous change in the input voltage and load torque. The treatment so far is based on a DC motor obtaining

its excitation separately. There are various forms of field excitation, discussed in the following section.

Exercise 1.1: DC Motor Starting Speed Response

A DC motor whose parameters are given in example 2.3 is started directly from a 220-V DC supply with **no load**. Find its starting speed response and the time taken to reach 100 rad s^{-1}

Solution

$$\frac{\omega(s)}{V(s)} = G_{\omega V}(s) = \frac{K_b}{s^2 (JL_a) + s (B_l L_a + JR_a) + (B_l R_a + K_b^2)} = \frac{15,968}{s^2 + 167s + 12874}$$

$$V(s) = \frac{220}{s}$$

$$\omega(s) = \frac{3.512 \times 10^6}{s(s^2 + 167s + 12874)}$$

$$\omega(t) = 272.8 \left[1 - 1.47 e^{-83.5 t} \sin(76.02t + 0.744) \right]$$

The time to reach 100 rad/sec is evaluated by equating the left-hand side of the above equation to 100 and solving for t , giving an approximate value of 10 rad/ms. ■

1.8. Field Excitation

The excitation to the field is **dependent on the connections of the field winding relative to the armature winding**. Based on how these connections are made, there are different configurations used in industry.

1.8.1. Separately Excited

If the field winding is physically and electrically separate from the armature winding, then it is known as a separately-excited DC machine, whose equivalent circuit is shown in **Fig. 1.6**.

The independent control of field current and armature current allows it to have simple but high performance control on this machine, as the torque and flux can be independently and precisely controlled.

The field flux (ϕ_f) is controlled **only** by the control of the field current (I_f).

For simplicity, assume that the field is constant. Then the torque is proportional only to the armature current,

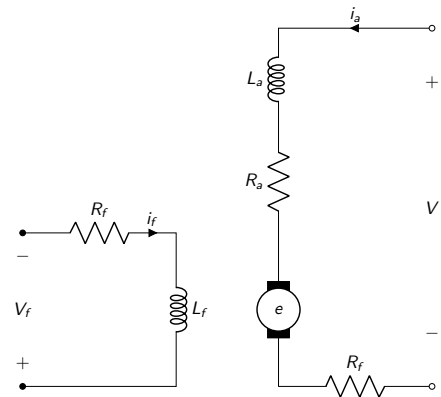


Figure 1.6: Circuit diagram of a separately-excited DC machine.

and, therefore, by controlling only this variable, the dynamics of the motor drive system can be controlled. With the independence of the torque and flux-production channels in this machine, it is easy to generate varying torques for a given speed, making torque generation independent of the operating speed.

This is an important operating feature in a machine: the speed regulation can be zero¹³. This can be done via a feedback control and via open-loop operation.

¹³This basically means the motor can sustain the same level of torque with varying speed and this is achieved by controlling the field current.

Exercise 1.2: Separately Excited DC - I

A separately-excited DC motor is delivering rated torque at rated speed. Find the motor efficiency at this operating point. The details of the machine are as follows:

$$\begin{array}{llll} 1500 \text{ kW}, & \text{Brush voltage drop} = 2 \text{ V}, & \text{rated current} = 2650 \text{ A}, & 600 \text{ rpm}, \\ 600 \text{ V}, & \text{Field power input} = 50 \text{ kW}, & R_a = 0.00364552 \text{ } \Omega, & L_a = 0.1 \text{ mH}, \end{array}$$

and the machine frictional torque coefficient = $51 \text{ N m rad}^{-1} \text{ s}$
Field current is constant and the armature voltage is variable.

Solution

To find the input power, the applied voltage to the armature to support a rated torque and rated speed has to be determined. In steady state, the armature voltage is given by

$$V_a = R_a I_{ar} + K_b \omega_{mr} + V_r,$$

where I_{ar} is the rated armature current, given as 2650 A, ω_{mr} is the rated speed in rad s^{-1} , and V_r is the voltage drop across the brushes in the armature circuit and is equal to 2 V as given by the problem. To solve this equation, the EMF constant has to be solved for from the available data. Recalling the torque and EMF constants being equal, the torque constant can be calculated from the rated electromagnetic torque and the rated current as

$$K_t = \frac{T_{er}}{I_{ar}} = \frac{T_s + T_f}{I_{ar}}$$

where the rated electromagnetic torque generated in the machine (T_{er}) is the sum of the rated shaft torque (T_s), and friction torque (T_f). The rated shaft or output torque is obtained from the output power and rated speed as follows:

$$\begin{aligned} \text{Rated speed } \omega_{mr} &= \frac{2\pi}{60} 600 = 62.83 \text{ rad s}^{-1} \\ \text{Rated shaft torque } T_s &= \frac{P_m}{\omega_{mr}} = \frac{1500 \times 10^3}{62.83} = 23,873 \text{ N m} \\ \text{Friction torque } T_f &= B_f \omega_{mr} = 51 \times 62.83 = 942.45 \text{ N m} \\ \text{Electromagnetic torque } T_{er} &= T_s + T_f = 23,873 + 942.45 = 24,815.45 \text{ N m} \end{aligned}$$

Therefore, the torque constant is:

$$\begin{aligned} K_t &= \frac{T_{er}}{I_{ar}} = \frac{24,815.45}{2650} = 9.364 \text{ N m A}^{-1} \\ K_b &= 9.364 \text{ V rad}^{-1} \text{ s} \end{aligned}$$

We can now calculate the input armature voltage as:

$$V_a = 0.003645 \times 2650 + 9.364 \times 62.83 + 2 = 600 \text{ V}$$

Armature and field power inputs:

$$V_a I_{ar} + \text{Field power input} = 600 \times 2650 + 50,000 = 1640 \text{ kW}$$

Therefore it's efficiency is:

$$\text{Efficiency} = \eta = \frac{P_m}{P_i} = \frac{1500}{1640} = 91.46\% \quad \blacksquare$$

1.8.2. Shunt Excited

If the field winding is connected in **parallel** to the armature winding, it is called **shunt-excited DC machine** or **DC shunt machine**. The equivalent circuit of the machine is shown in **Fig. 1.7**.

The field winding does not need a separate power supply, as it does in the case of the separately-excited DC machine.

For a constant input voltage, the field current and hence the field flux are constant. While it is good for a constant-input-voltage, the propagation of the current is constant. In variable-input voltage is proportional to the voltage of the radiation and field currents is lost, leading to a coupling of the flux and torque production channels in the machine. This is in contrast to the control simplicity of the separately-excited DC machine. For a fixed input voltage, the electromagnetic torque is v -speed characteristic of the DC shunt machine is shown in Figure 2.6. As torque is increased, the magnetic moment is the same, and hence the armature voltage drop also increases, while at the same time, the speed is decreased. The reduction in the induced EMF is reflected in a lower speed, since the field current is constant in the machine. The drop in speed from its no-load speed is relatively small, and, because of this, the DC shunt machine is considered a constant-speed machine. Such a feature makes it unsuitable for variable-speed application.

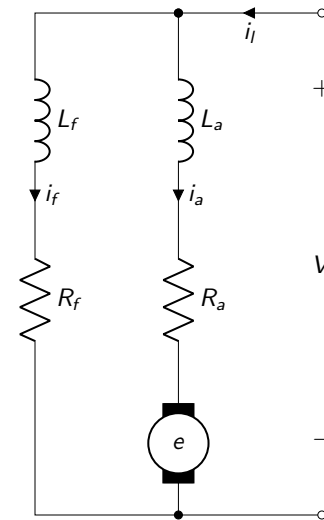


Figure 1.7.: Circuit diagram of a shunt-excited DC machine.

1.8.3. Series Excited

If the field winding is connected in series with the armature winding, then it is known as the *series-excited DC machine* or *dc series machine*, and its equivalent circuit is shown in **Fig. 1.8**.

It has similar disadvantages as the shunt machine, as there is **no independence** between the control of the field and the armature currents. The electromagnetic torque of the machine is proportional to the square of the armature current, as the field strength is equal to the armature current.

At low speeds, a high armature current is possible, with

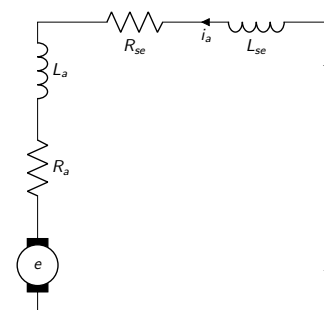


Figure 1.8.: Circuit diagram of a series-excited DC machine.

a large difference between a fixed applied voltage and a small induced EMF. This results in high torque at starting and low speeds, making it an ideal choice for applications requiring high starting torques, such as a propulsion.

With the dependence of the torque on the square of the armature current and the fact that the armature current availability goes down with increasing speed, torque-vs-speed characteristic resembles a hyperbola.

At zero speed and low speeds, the torque is large but somewhat curtailed from the square current law because of the saturation of the flux path with high currents.

1.8.4. Compound

Combining the best features of the series and shunt DC machines by having **both a series and shunt field** in a machine leads to the **dc compound machine** [10], shown in **Fig. 1.9**. The manner in which the shunt-field winding is connected in relation to the armature and series field provides two (2) kinds of compound DC machine [11].

- If the shunt field encompasses the series field and armature windings, then that configuration is known as long-shunt compound DC machine.
- If the shunt field encompasses only the armature winding it is called short-shunt compound DC machine.

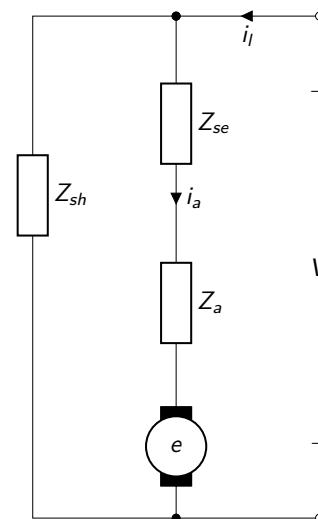


Figure 1.9.: Circuit diagram of a separately-excited DC machine.

Whether the field fluxes of the shunt and series field are opposing or strengthening each other gives two (2) other configurations, known as [12]:

- differential compound,
- cumulatively compound

respectively, for each of the long and short shunt connections.

1.8.5. Permanent-Magnets

Instead of an electromagnet with an external DC supply, the excitation can be provided by PMs such as ceramic, aninco, and others¹⁴. The advantage of such an excitation consists in the compactness of the field structure and elimination of resistive losses in the field winding. These features contribute

¹⁴These will be covered in Chapter ?? in significant detail.

to a compact and ,temperature-wise, cooler machine, desirable features for a high-performance motor.

the armature is similar to other DC motors in construction and performance.

1.9. Measuring the Motor Constants

To analyze a DC motor, the constants R_a , L_a and K_b and the resistance and inductance of field windings are required. Some of them are given in the manufacturers' data sheets. In case of nonavailability of the data, it is helpful to have knowledge of procedures to measure these constants.

In this short digression we will have a look at the test methods to a separately excited dc motor¹⁵.

1.9.1. Armature Resistance

Armature, if you recall is the part where AC current flows, in which chase for DC motor is the rotor. The DC value of the armature resistance is measured between the armature terminals by applying a DC voltage to circulate rated armature current.

It is important to subtract the brush and contact resistance from the measurement and to correct for the temperature at which the motor is expected to operate at steady state.

1.9.2. Armature Inductance

By applying a low AC voltage through a variac¹⁶ to the armature terminals, the current is measured. The motor has to be at a standstill, keeping the induced EMF at zero.

Permeability, the residual voltage in the machine is wiped out by repetitive application of positive and negative DC voltage to the armature terminals.

The test schematic is shown in Figure 2.11. The inductance is

$$L_a = \frac{\sqrt{(V_a^2/I_a) - R_a^2}}{2\pi f_s}$$

where f_s is the frequency in Hz and the armature resistance has to be the AC resistance of the armature winding.

This is different from the DC resistance, because skin effect¹⁷ produced by the alternating current.

¹⁵The reason as why this motor was chosen instead of other types is that it is the most widely used motor for variable-speed applications.

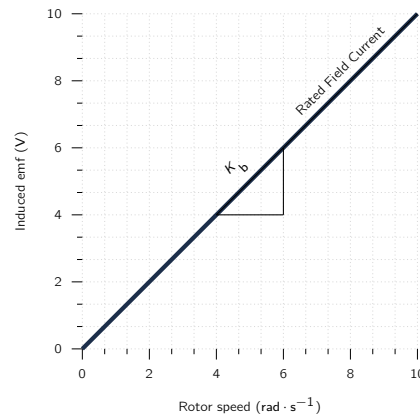
¹⁶A type of autotransformer that provide adjustable AC voltage.

¹⁷The tendency of AC to become distributed within a conductor such that the current density is largest near the surface of the conductor and decreases exponentially with greater depths in the conductor.

1.9.3. EMF Constant

Rated voltage¹⁸ is applied and kept constant, and the shaft is rotated by a prime mover (another DC motor) up to the speed given in the name plate (called rated speed or base speed).

The armature is open-circuited, with a voltmeter connected across the terminals. The voltmeter reads the induced EMF, and its readings are noted for various speeds and are plotted as shown in **Fig. 1.10**. The slope of this curve at a specific speed gives the EMF constant in volt-sec/rad as seen from Eq. (1.3). The relationship shown in **Fig. 1.10** is known as the open-circuit characteristic of the DC machine¹⁹.



¹⁸Also known by some engineering wizards as specific field voltage.

¹⁹for a permanent-magnet machine, this procedure is not applicable.

Figure 1.10.: Induced EMF v. rotor speed characteristics at rated field current.

1.10. Simulation

Based on previous knowledge, let's do a simulation of a separately-excited DC machine. For this we will use OpenModelica.

1.10.1. Separately-Excited

The model for the simulation is given in **Fig. 1.11**. As can be seen there are a few things which are worth discussing. First is we need to turn on the motor, for that we employ a ramp function which increases the armature voltage in a linear fashion²⁰.

Second aspect is the introduction of a load. While it is true that the motor has inherent inertial

²⁰Think of this as someone slowly turning down a potentiometer to slowly start a machine.

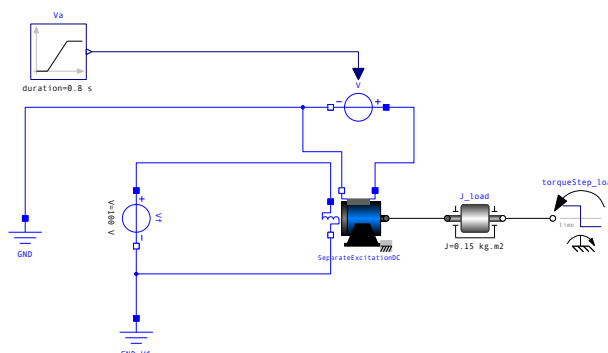


Figure 1.11.: The simulation diagram of a separately excited DC machine.

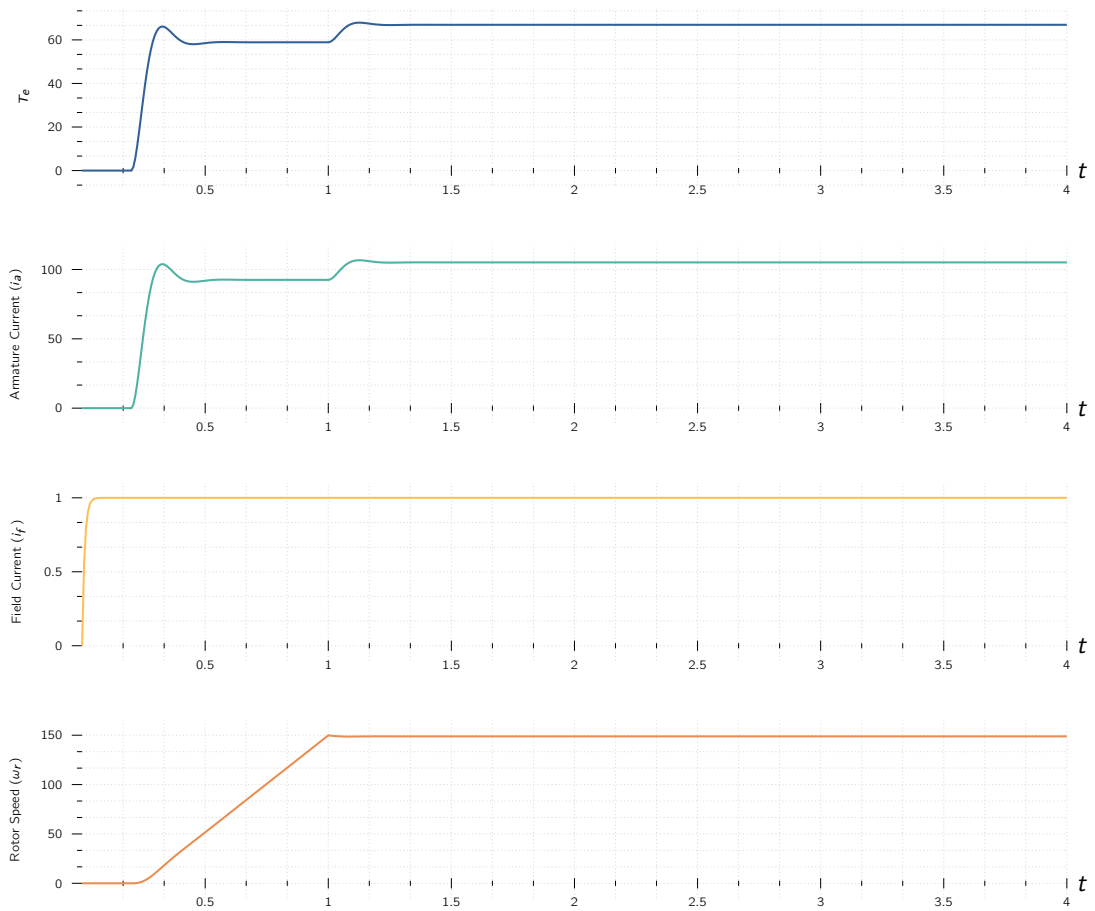


Figure 1.12.: Simulation Results of the separately-excited DC motor.

load, as it is spinning the rotor, an additional load is introduced to study it's dynamics when sudden change in load occurs.

Parameter	Value	Symbol	Parameter	Value	Symbol
Field Voltage	100	V	Armature Voltage	100	V
Field Resistance	100 Ω	R_f	Armature Resistance	0.05 Ω	R_a
Field Inductance	1 H	L_f	Armature Inductance	0.0015 H	L_a
Nominal Armature Voltage	100 V	$V_{a(nom)}$	Nominal Armature Current	100 A	$I_{a(nom)}$
Nominal Rotor Speed	1425 rpm	$\omega_{r(nom)}$	Rotor Inertial Load	0.15 kg m^{-2}	J_r
Torque Step	-66.93 N m	T_{step}	Torque Step start-time	1 s	t_{torque}
Ramp duration	0.8 s	$t_{ramp(dur)}$	Ramp start time	0.2 s	$t_{ramp(start)}$

Table 1.1.: Simulation parameters for the separately-excited DC motor.

The results are shown in the following section.

Let's have a look at the results. As we can see the field current has an almost instant but a delayed response. This is caused by the field inductance having a delayed response to the current²¹. The current does not change with regards to the load as the field is **independent** from the load of the rotor.

²¹While in steady-state the entire system can be analysed as a DC, in transient behaviour the AC properties **must** be taken into account.

Some of you who may be observant may ask about the effect of the armature reaction on the field current. While the effect can be noticeable the complexity of mathematical modelling is not justified for the accuracy one would get from implementing it.

Another important factor to mention is the **proportional relationship** between the generated electromagnetic torque and the armature current. As can be seen one is just a direct proportion of another. The machine with its internal load (J_r) stabilises at around 60 N m but once the new load is introduced, the machine has increased the torque production and with it, it is drawing even higher current from the grid.

Final thing to consider is the rotational speed (ω_r). Here without the load the motor is reaching around 1500 rpm, which is higher than its defined nominal operational speed²². Once the significant load is introduced, the rotor speed stabilises to its nominal value.

²²This is due to the fact that the machine, when designed, assumes a load to be operated upon and its nominal speed is calculated based on that.

Part II.

Induction Machines

Chapter 2

Induction Motor Dynamics and Control

Table of Contents

2.1. Introduction	23
2.2. Steady-State Analysis	24
2.3. Construction	27
2.4. Dynamic Modelling	33
2.5. Dynamic Simulation Equations	50

2.1. Introduction

An IM is type of electro-mechanical device¹ whereby AC is supplied to the stator **directly** and to the rotor by **induction** from the stator, when excited from a balanced poly-phase source². During operation, it will produce a magnetic field in its air gap rotating at **synchronous speed** as determined by the number of stator poles and the applied stator frequency f_e which can either be fed from the grid or from an inverter. A cross sectional view of an IM can be seen in **Fig. 2.1**.

IMs are the go-to choice for AC machines in industry [14] and are a commonplace in a wide variety of applications such as mining [15, 16], power generation [17], and electric cars [18]. The benefits of IM over other types is its optimised construction, cheap production, and simple construction. Therefore the understanding

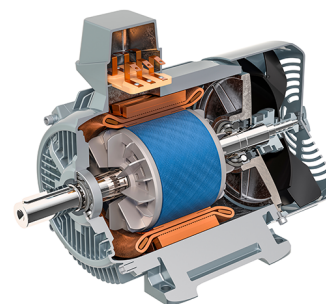


Figure 2.1.: Cross-sectional view of IM [13].

¹some consider it as a rotating transformer

²either by star or delta connection if it is a three-phase connection, however there are applications which $ph > 3$ is used, which are in places where high traction is needed.

of its behaviour and modelling its dynamics is useful if not essential.

³known in literature as $dq0$ axes [19].

In this section, the dynamic model of the IM in direct-quadrature, and zero-sequence axes³ is derived from fundamentals.

To simplify the problems we will face in modelling an AC system we will use certain transformations. These transformations used in the derivation of various dynamic models are based on simple trigonometric relationships obtained as projections on a set of axes⁴. The dynamic model is derived with the frames of the observation starting at an arbitrary speed. The same idea is used to obtain transient responses, small-signal equations, and a multitude of transfer functions, all of which are useful in the study of converter-fed induction-motor drivers [21]. Space-phaser approach has further simplified the polyphase IM model to one equivalent stator and one rotor winding, thereby evolving a powerful similarity to the DC machine to correspond with its armature and field windings⁵.

⁴A direct, and a quadrature axis.

⁵This is the main goal of any AC machine analysis: to create a mathematical analogy with a DC machine.



Figure 2.2.: A wound-rotor IM [20].

2.2. Steady-State Analysis

The rotor of a poly-phase IM may be one of two (2) types⁶.

Wound Rotor built with a polyphase winding similar to, and wound with the same number of poles as, the stator. The terminals of the rotor winding are connected to insulated slip rings mounted on the shaft. Carbon brushes bearing on these rings make the rotor terminals available external to the machine, which can be seen in Fig. 2.2.

Wound-rotor IM are relatively uncommon, being found only in a limited number of specialised applications where good control of speed is required.

Squirrel Cage rotor windings consist of conducting bars embedded in slots in the rotor iron and short-circuited at each end by conducting end rings⁷. The extreme simplicity, ruggedness, and a century of industrial optimisation makes the squirrel-cage construction the dominant type of IM ranging from a less than a kW to a MW.

⁷These bars are usually made from aluminium or copper.

2.2.1. Speed of Operation

To understand the operation principle of an IM, let us assume the rotor is turning at the steady speed of n_r rpm in the same direction as the rotating stator field. Let the synchronous speed of the

stator field be n_s rpm. This difference between synchronous speed and the rotor speed is commonly referred to as the **slip** of the rotor⁸.

Slip is more usually expressed as a fraction of synchronous speed⁹.

⁸For more information, please look at the B.Sc Drive Technology Repo.

⁹i.e., 0 – 100 %

The **fractional slip**, ranging between 0 and 1, (s) is:

$$s = \frac{n_s - n_r}{n_s} \quad (2.1)$$

The slip is often expressed in percent (%), simply equal to 100 percent times the fractional slip of Eq. (2.1) whereas the rotor speed in rpm can be expressed in terms of the slip and the synchronous speed as:

$$n_r = (1 - s) n_s \quad (2.2)$$

Similarly, the mechanical angular velocity (ω_r) can be expressed in terms of the synchronous angular velocity (ω_s) and the slip as:

$$\omega_r = (1 - s) \omega_s \quad (2.3)$$

A final relationship could be made with regards to the stator frequency (f_s) and rotor frequency (f_r):

$$f_r = s f_s \quad (2.4)$$

The electrical behaviour of an IM is similar to a transformer but with the additional feature of **frequency transformation** produced by the relative motion of the stator and rotor windings. A useful application of wound-rotor IM is as a frequency changer as the frequency of the rotor and the stator is **different**.

Starting Up the Motor

The terminals of an squirrel-cage IM rotors are **internally short circuited** whereas in a wound-rotor IM it is short circuited **externally**. The rotating air-gap flux induces slip-frequency voltages in the rotor windings. The rotor currents are then determined by the magnitudes of the induced voltages and the rotor impedance at slip frequency.

During startup, the rotor is stationary ($n_r = 0$), the slip is **unity** ($s = 1$), and the rotor frequency equals the stator frequency (f_s). The field produced by the rotor currents therefore revolves at the same speed as the stator field, and a starting torque results, ending to turn the rotor **in the direction of the stator field rotation**. If this torque is sufficient to overcome the opposition to rotation created by the shaft load, the machine will come up to its operating speed.

The operating speed can never equal the synchronous speed as the rotor conductors would then be stationary **with respect to** the stator field; no current would be induced in them, and therefore no torque would be produced.

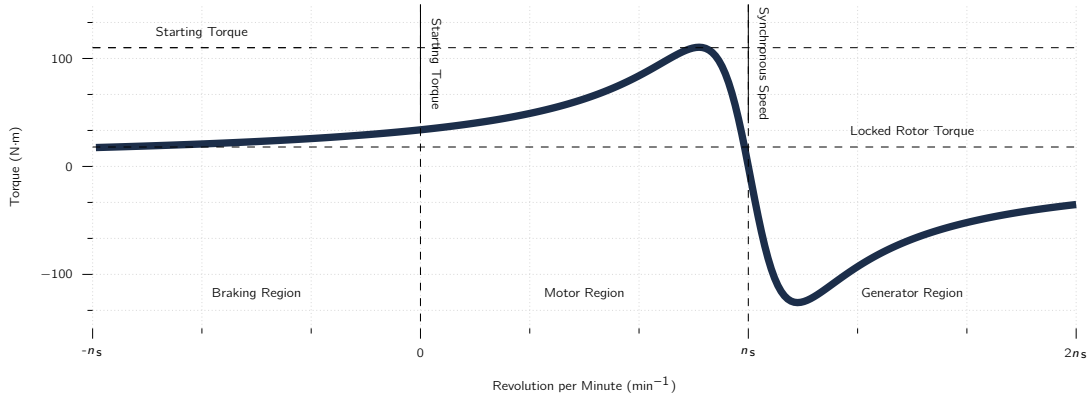


Figure 2.3.: Steady-state torque behaviour of an IM. Here important parameters and concepts can be observed. An important aspect is to mention is the stability of an IM only occurs between %2 to %8 slip during normal operation.

With rotor revolving in the same direction of the stator field, the frequency of the rotor currents is sf_s and they will produce a rotating flux wave which will rotate at sn_s rpm with respect to the rotor in the forward direction. But superimposed on this rotation is the mechanical rotation of the rotor at n rpm.

Therefore, with respect to the stator, the speed of the flux wave produced by the rotor currents is the sum of these two (2) speeds and equals

$$sn_s + n_r = sn_s + n_s(1 - s) = n_s \quad (2.5)$$

From Eq. (2.5) we see the rotor currents produce an air-gap flux wave which rotates at synchronous speed and is synchronised with that produced by the stator currents. Because the stator and rotor fields each rotate synchronously, they are stationary with respect to each other and produce a steady torque, thus maintaining rotation of the rotor. Such torque, which exists for any mechanical rotor speed n_s other than synchronous speed, is called an **asynchronous torque**.

2.2.2. Normal Operation

Under normal running conditions the slip s is small¹⁰. As the rotor frequency is directly related to slip the frequency ($f_r = sf_s$) of the current flowing in the rotor is very low, around 1 to 5 Hz in 50-Hz machines. In this range the rotor impedance is **largely resistive and independent of slip**, as reactance element is proportional to $2\pi f_r L$.

Approximate proportionality of torque with slip is therefore to be expected in the range where the slip is small. As slip increases, the rotor impedance increases due to the increasing contribution of the rotor leakage inductance. Therefore, the rotor current is less than proportional to slip. The result is that the torque increases with increasing slip up to a maximum value and then decreases. The maximum torque, or **breakdown torque**, which is typically a factor of two larger than the rated machine torque, limits the short-time overload capability of the machine.

¹⁰2 to 10 percent at full load in most squirrel-case IMs

The slip at which the peak torque occurs is proportional to the rotor resistance.

For squirrel-cage machines this peak-torque slip is relatively small. Therefore, the squirrel-cage IM is substantially a constant-speed machine having a few percent drop in speed from no load to full load. In the case of a wound-rotor IM, the rotor resistance can be increased by inserting external resistance, hence increasing the slip at peak-torque, and thus decreasing the machine speed for a specified value of torque. The speed-torque plot of a squirrel-cage IM can be seen in **Fig. 2.3**.

Wound-rotor¹¹ IM are generally made to be larger, and therefore are more expensive and require significantly more maintenance than squirrel-cage IMs, this method of speed control is rarely used, and IMs driven from constant-frequency sources tend to be limited to essentially constant-speed applications.

¹¹While wound-rotor has significant merits compared to that of a squirrel-cage the market-share is around %5 compared to squirrel-cages' %95. Therefore, the dynamic modelling usually takes a squirrel cage into account.

2.3. Construction

Magnetic Part

The stator and rotor of IM are made up of magnetic steel laminations of thickness varying from 0.0185 to 0.035 inch¹², machine-punched with slots at the inner periphery for the stator and at the outer periphery for the rotor [23] which can be seen in **Fig. 2.4**. These slots can be partially closed or fully open in the stator laminations to adjust the leakage inductance¹³ of the stator windings. In the rotor dimensions, the stator can be arbitrarily small enough to move from the rotor. The rotor stops can be seen as the path length of the rotor.



¹²0.47 to 0.875 mm

¹³an inductive component that results from the imperfect magnetic linking of one winding to another

Figure 2.4.: Lamination on a stator is done to reduce eddy currents [13].

The rotor will cross-part networks to be bold rotor bars of different shapes placed in them. In such a case, the rotor is known as a deep bar rotor. Depending on the number of parallel copper bars placed in a slot, the machine is referred to as a double-, triple-, or multiple-age IM.

The multiple-cage rotor is intended to maximise the electromagnetic torque during starting and to minimise the rotor copper losses during steady-state operation. The stator laminations are aligned and stacked in a future and pressed by heavy presses of capacity varying from 40 to 80 tons, to pack the laminations very closely and to remove the air gap between them. With these steps, the stator magnetic part of the machine is ready for insertion of windings [24].

The rotor windings are **skewed** by one half or a full slot pitch from one end to the other, to minimise or to completely cancel some of the time harmonics¹⁴. To accommodate such skewing, the rotor laminations are assembled with a skew in a jig and fixture and then pressed to make the rotor magnetic block [25, 26].

¹⁴harmonics in the input supply given to the three phase machine.

Windings

Stator & Rotor Windings

Consider a three-phase IM having three (3) windings each on its stator and rotor. The phase windings are displaced in space from each other by 120° electrical degrees¹⁵, where

¹⁵or $\pi/3$ if you prefer radians.

$$\text{Electrical degrees} = \text{Pairs of poles} \times \text{Mechanical degrees} \quad (2.6)$$

The three-phase rotor windings are **short-circuited** either within the rotor or outside of the rotor, with or without external resistances connected to them. If the rotor windings are connected through slip rings mounted on the shaft and adjacent to the rotor of the IM to provide external access to the rotor windings, the machine is referred to as a **slip-ring induction** motor, as mentioned previously. Alternately, the rotor windings can be bars of copper or aluminium, with two (2) end rings attached to short-circuit the bars on the rotor itself, thus making the rotor very compact [27]. Such a construction is known as **squirrel-cage IM**.

The numbers of slots in the stator and rotor are unequal to avoid harmonic crawling torques¹⁶ [29]. The windings are distributed in the slots across the periphery of the stator and rotor. The windings can have different progressions, such as **concentric** or **lap** windings. In concentric windings, the windings are centred around slots within a pole pitch. In the case of lap windings, a coil is spread over a fixed pitch angle, for example, 180 electrical degrees, and connected to the coil in the adjacent slot, and so on. With a coil pitch of 180 electrical degrees, the induced EMF of the coil side under the south pole. The inductance of the coil is equal to the sum of the incidence of the rotor. The induced emf in the coil is equal to the sum of the incidence of the coils. The winding number of the coil is equal to the sum of the coils. The windings need not have a pitch of 180 electrical degrees and might have less than that, to eliminate some fixed number of harmonics. This case is known as short-chorded winding. Short chording reduces the resultant voltage, because the coils are not displaced by 180 degrees but by less, with the outcome that their phasor sum is less than their algebraic sum. Such an effect is included in the **pitch factor**, c_p .

The slots have a phase shift, both to allow for mechanical integrity and to control the short-chording angle, so the induced EMF in the adjacent coils of a phase will have a phase displacement. When the EMF is the noise coils of a phase are summed up, the resultant induced EMF is the sum of the phasor voltages induced in the tensile coils. A reduction in the voltage results because of the phasor addition compared to their algebraic sum. The factor to account for this aspect is known as the **distribution factor**, c_d . The resultant voltage in a phase winding is reduced both by the pitch and distribution factors. Therefore, the winding factor, k_w , which reflects the effectiveness of the winding, is given as:

$$k_w = c_d c_p,$$

where c_d is the winding distribution factor.

¹⁶This action is due to the fact that harmonics fluxes are produced in the gap of the stator winding of odd harmonics like 3rd, 5th, 7th, etc. These harmonics create additional torque fields in addition to the synchronous torque [28].

Induced EMF

With this understanding, the induced EMF in a stator phase winding is derived from the first principles¹⁷. The mutual flux linkages are distributed **sinusoidal**. The induced EMF is equal in magnitude to the rate of change of mutual flux linkages, which in turn is equal to the product of the effective number of turns in the winding and the mutual flux.

¹⁷In this case we derive it from Faraday's law taught in M.Sc Electrodynamics.

From this, the induced EMF in a phase winding is derived as:

$$e_{as} = -\frac{d\lambda}{dt} = -\frac{d}{dt} \left[(k_{w1} T_1) \Phi_m \sin(2\pi f_s t) \right] = -2\pi f_s k_{w1} T_1 \Phi_m \cos(2\pi f_s t),$$

where f_s is the supply frequency in Hz, Φ_m is the peak value of the mutual flux, T_1 is the total number of turns in phase a , and k_{w1} is the stator winding factor. The rms value of the induced emf is given by

$$E_{as} = \frac{|e_{as}|}{\sqrt{2}} = 4.44 k_{w1} T_1 \Phi_m f_s \quad (2.7)$$

The expression for the induced EMF in the rotor phase windings is very similar to Eq. (2.7) if appropriate winding factor, number of turns, and frequency for the induced EMF in the rotor are inserted into Eq. (2.7).

Winding Methods

There are two (2) types of winding methods are common in IMs.

- Random-wound,
- Form-wound.

Let's look at them in a bit more detail:

Random-Wound Winding

The coils are placed in the slots and separated from the magnetic steel with an insulation paper, such as a mined short, which can be see in **Fig. 2.5**. Each coil in a slot contains a number of circular but stranded emptied wires which are wound on a former. This type of winding is referred to as random-wound. They are used for low-voltage (< 600 V) motors. The disadvantages of this method of winding the coil are:

- The adjacent round wires in the worst case can be the first and the last turn in the coil. Because of this, the turn-to-turn voltage can be maximum in such a case and will equal the full coil voltage but not equal the sequential turn-to-turn voltage, which is only a small fraction of the full coil voltage.

- They are likely to have considerable air pockets, the full coil voltages. These air pockets form capacitors between strands of wire. With rotational of repetitive voltages at high frequency with high rate of change of voltages from the inverter, a discharge current flows into the air capacitor. This is known as partial discharge and can cause insulation failures.

However, random-wound machines are economical, have low losses, and hence have a higher efficiency and tend to run cooler, Random-wound machines use a semi-closed slot, which reduces the flux density in the teeth, resulting in lower core losses¹⁸. Some methods have very recently been suggested to reduce the partial-discharge possibility of random-wound machines.

¹⁸ This can be as much as 20 to 30%

The methods recommend using:

- heavier insulation,
- a wind-in-place insertion method, making the wire placement sequential
- extra strategically placed insulation within a phase of the motor
- extra insulating steves on the turns nearer to the line leads

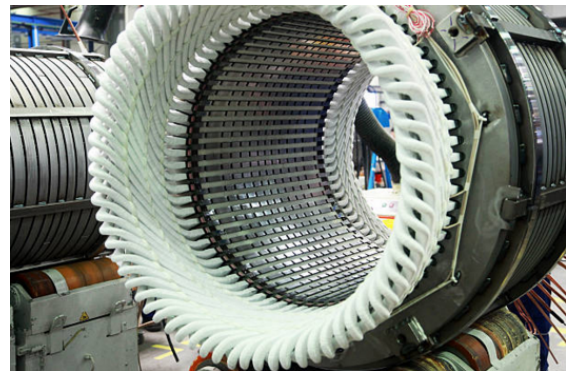


Figure 2.5.: Form winding.

Form-Wound Winding

Higher-voltage (>600 V) IMs are usually wound in form, meaning, each wire of rectangular cross section is placed in sequence with a strand of insulation in between them and then the bundle is wrapped with mica ground wall insulation, over which an armour covering is applied to keep all the wire arrangement firmly in place. The form-wound coils are placed in a fully open slot, as it is not possible to use the semi-closed slot for this arrangement.

This wound has higher higher core losses.

This is because the tooth flux density increases as there is a sizable reduction of its cross sectional area compared to a semi-closed slotted tooth. On the other hand, form-wound windings have a much higher resistance to partial discharges, as their turn-to-turn voltage is minimal and a heavier insulation bound between them also helps mitigate them.

The disadvantage of this winding is that it is relatively expensive compared to random windings.

Rotor Construction

There are two (2) methods of rotor construction are used for IMs. They are fabrication and die casting of the rotor. Fabricated rotor construction is possible for both aluminium and copper bar rotors but aluminium fabricated rotors are hardly ever used.

The reason is that a fabricated aluminium rotor is expensive, whereas a die-cast aluminium rotor is inexpensive.

The fabricated copper-bar rotor is used in large machines where the aluminium die-cast rotor is not available or in high-inertia loads demanding frequent starts, such as in crushers and shredders. Frequent line-supply starts of the IM result in higher-inrush currents¹⁹ that are multiple times the rated currents and hence produce more losses and forces capable of disclosing the rotor bars.

¹⁹the high current a highly inductive load draws when it is first energised.

The aluminium die-cast rotor construction is used in applications having lower-load inertia than recommended by National Electrical Manufacturers Association (NEMA) and **NOT** required to meet stall condition or very high starting torques [30].

This rotor type is dominant in applications and covers as much as 90% of applications.

Insulation

Wounded stator and rotor windings are immersed in varnish and heat-treated for drying. The insulation sheets between slots and coils and on the enamelled²⁰ wires and between turns in the coil consist of insulation materials of different classes, known as **A**, **B**, **F**, and **H**. The choice depends on the maximum temperature rise permissible for each class. The NEMA [MG1](#) and American National Standards Institution (ANSI) [CR50.41](#) specifies for allowable stator temperature rise for various insulation classes, with the European standard regulated by International Electrotechnical Commission (IEC) 60034-1:2022 [31].

²⁰enamelling is the process of applying varnish on the surface of copper or aluminium wires to form electrical insulation film. This process also increases mechanical strength, thermal resistant and chemical resistant properties.

Service factor is the ratio between the steady-state maximum power output capability and the rated power output of the machine. As an example, a service factor of 1.15 means the machine can practically generate %15 more power than what is written on its nameplate.

Because of the uncertainty of measuring certain loads, service factor greater than 1 is recommended in field applications.

most IM have insulation class **F**, whereas motors for servo-drive applications usually need class **H** insulation.

If the machine is not going to be in constant operation or has no overload application, lower class insulation can be chosen to save on cost.

Higher winding temperatures usually result in transmission of heat to bearings, resulting in failures and frequent replacements. Therefore, higher operating winding temperature is not preferred, and that is the reason for a majority of motors to have an insulation class of **F** or lower.

Rotor Shaft

The rotor shaft is usually made of **forged steel** for higher speeds (i.e., $n_r > 3600$ rpm) and has to conform to sizes recommended for power levels by NEMA or other applications-specific industrial standards such as American Petroleum Institute (API) standard [541](#) for American markets and IEC 60072-1:2022 [32] for European.

Enclosure

Windings are inserted in the stator laminations and the stator laminations are fitted inside of a non-magnetic steel housing. Two end covers will be attached to the steel housing with part of the bearings attached to them. They then will be assembled with through bolts after inserting the rotor with shaft. The non-magnetic steel housing is intended for protecting the stator and rotor assembly from an inertial forces²¹. Commonly used enclosures are:

²¹such as pin, water, snow, insect, birds, ...

- open dip-proof (ODP)
- weather-protected types I and II (WPLWPI)
- totally enclosed air-to-air cooled (TEAC),
- totally enclosed fan cooled (TEFC),
- totally enclosed water-to-air cooled (TEAC)

These provide varying degrees of protection from environment and core with cost different widely between them.

Rotor Balancing

Before final assembly, the rotor is dynamically balanced so no eccentricities of any kind are presented to the bearings. The balancing is achieved either by **removing some magnetic iron material** in smaller motors or by **adding a magnetically and electrically inert material** compound in larger machines. To close this topic of, here is a diagram showing the materials generally used in the construction of the IM, shown in **Fig. 2.6**.

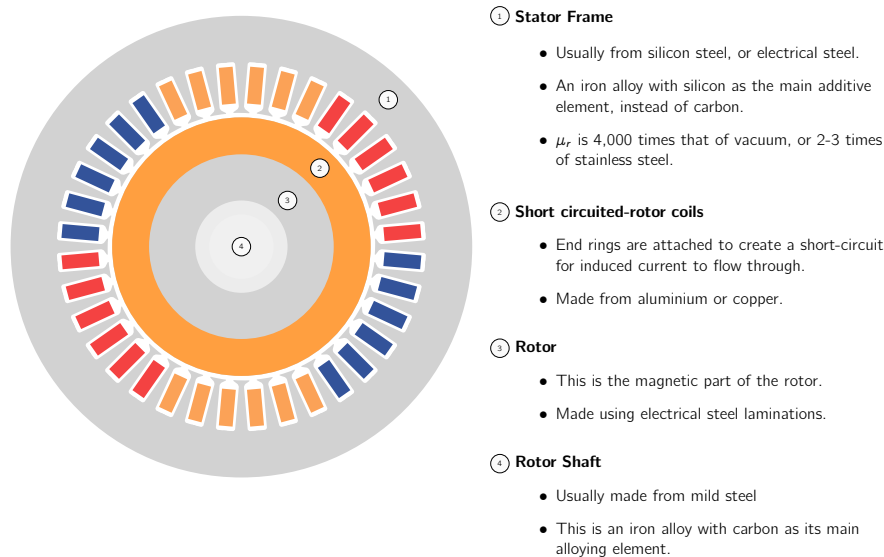


Figure 2.6.: The materials used in the construction of an IM.

2.4. Dynamic Modelling

The steady-state model and equivalent circuit developed in **B.Sc Drive Technology** are useful for studying the performance of an IM in **normal operation**. This implies all electrical transients are **neglected** during load changes and stator frequency variations. Such variations arise in applications involving variable-speed drives.

The variable-speed drives are converter-fed from finite sources, unlike the utility sources, due to the limitations of the switch ratings and filter sizes.

This results in their incompatibility to supply large transient power. Therefore, it is in our best interest, to evaluate the dynamics of converter-fed variable-speed drives to assess the adequacy of the converter switches and the converters for a given motor and their interaction to determine the excursions of currents and torque in the converter and motor.

The dynamics model considers the three (3) major properties of an IM:

1. instantaneous effects of varying voltages/currents,
2. stator frequency, and
3. torque disturbance.

The dynamic model of the IM is derived using a two-phase motor in direct and quadratic (**d, q**) effects. This approach is desirable because of the conceptual simplicity obtained with two (2) sets of windings, one on the stator and the other on the motor.

For this transformation to work we need to introduce the concept of **power invariance**; the power

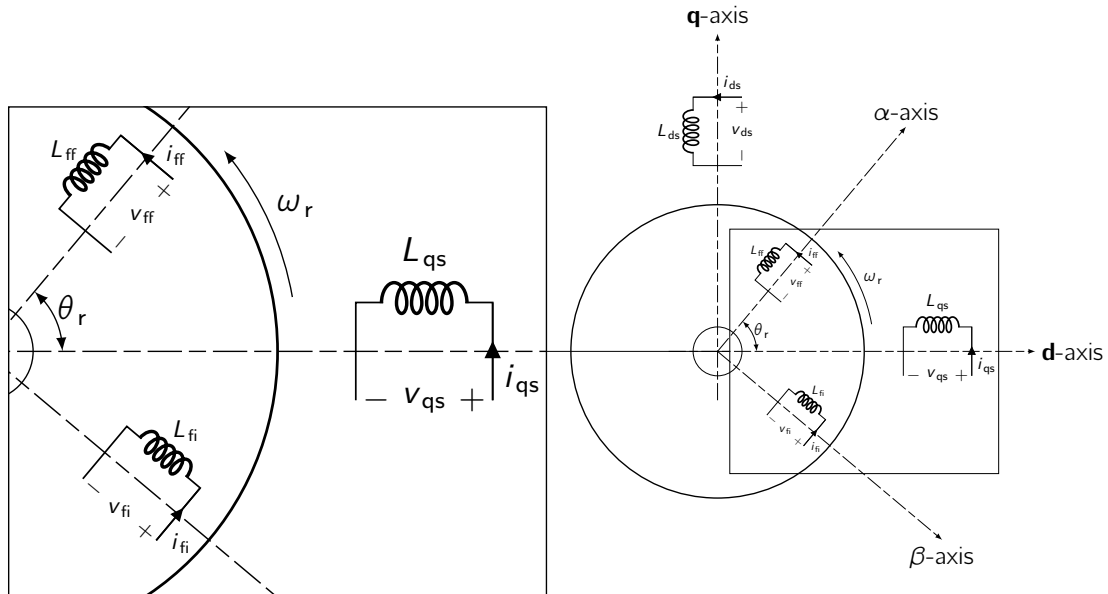


Figure 2.7.: Stator and rotor winding of a two-phase IM. The model shows the stator inductances as L_{qs} and L_{ds} , and the rotor as L_{α} and L_{β} . as the rotor spins these inductances will interact with one another and produce mutual inductance.

must be equal in the three-phase machine and its equivalent two-phase model. The required transformation in voltages, currents of flux linkages is derived in a generalised way. The reference frames are chosen to be **arbitrary**, and particular cases such as stationary, rotor, and synchronous reference frames, are simple instances of the general case. Deviations for electromagnetic torque involving the currents and flux-linkages are given.

The differential equations describing IM are **non-linear**. For stability and designing controllers it is important to linearise the machine equations around a steady-state operating point to obtain small-signal equations. Time to start derive the two-phase equivalent model.

2.4.1. Real Time Model of a Two-Phase Induction Machine

The following assumptions are necessary to derive the dynamic model²²[33]:

- The machine has **uniform air gap** (i.e., δ is constant across circumference),
- Balanced rotor and stator windings with sinusoidally distributed MMF. This permits us to assume the system to be void of any **spatial harmonics**.
- Inductance v. rotor position is sinusoidal²³.
- Saturation and parameter changes are neglected (i.e., material is assumed linear)

A two (2) phase IM with stator and rotor windings is shown in **Fig. 2.7**. The windings are displaced in space by 90° electrical, and the rotor winding, α , is at an angle θ_r , from the stator **d** axis winding.

²²These assumptions allow us to disregard non-symmetrical geometries or non-linear behaviour of materials.

²³This is just another way of saying we are working with cylindrical symmetric bodies and not salient poles.

It is assumed that the d-axis (**d**) is **leading** q-axis (**q**) for clockwise direction of rotation of the rotor. If the clockwise phase sequence is **dq**, the rotating magnetic field will be revolving at the angular speed of the supply frequency but counter to the phase sequence of the stator supply. Therefore, the rotor is **pulled in the direction of the rotating magnetic field**. For this case it is counter-clockwise. The currents and voltages of the stator and rotor windings are marked in **Fig. 2.7**. The number of turns per phase in the stator and rotor windings respectively are T_1 and T_2 .

A pair of poles is assumed for **Fig. 2.7**, but it is applicable with the slight modification for the rotation of the rotor position at drawn in terms of electrical heterogeneity.

θ_r is the electrical rotor position at any instant, obtained by multiplying the rotation of the rotor position by pairs of electrical poles.

The terminal voltages of the stator and rotor windings can be expressed as the sum of the voltage drops in resistances and rates of change of flux linkages, which are the products of currents and inductance [34].

The equations are as follows:

$$v_{qs} = R_q i_{qs} + p_t (L_{qq} i_{qs}) + p_t (L_{qd} i_{ds}) + p_t (L_{q\alpha} i_{\alpha}) + p_t (L_{q\beta} i_{\beta}) \quad (2.8)$$

$$v_{ds} = p_t (L_{dq} i_{qs}) + R_d i_{ds} + p_t (L_{dd} i_{ds}) + p_t (L_{d\alpha} i_{\alpha}) + p_t (L_{d\beta} i_{\beta}) \quad (2.9)$$

$$v_{\alpha} = p_t (L_{\alpha q} i_{qs}) + p_t (L_{\alpha d} i_{ds}) + R_{\alpha} i_{\alpha} + p_t (L_{\alpha\alpha} i_{\alpha}) + p_t (L_{\alpha\beta} i_{\beta}) \quad (2.10)$$

$$v_{\beta} = p_t (L_{\beta q} i_{qs}) + p_t (L_{\beta d} i_{ds}) + p_t (L_{\beta\alpha} i_{\alpha}) + R_{\beta} i_{\beta} + p_t (L_{\beta\beta} i_{\beta}) \quad (2.11)$$

where p_t is the **short-hand notation** for the differential operator²⁴ d/dt , and the various inductances are explained as follows:

²⁴Which makes this a system of ODEs, if we recall **Higher Mathematics I**.

- $v_{qs}, v_{ds}, v_{\alpha}, v_{\beta}$ are the terminal voltages of the stator **d** axis, **q** axis, and rotor α and β windings respectively.
- i_{α}, i_{β} are the rotor α, β winding currents respectively.
- $L_{qq}, L_{dd}, L_{\alpha\alpha}, L_{\beta\beta}$ are the stator **d**, and **q** axis winding and rotor α and β winding self inductances respectively.

The mutual inductances between any two (2) windings are denoted by L with two (2) subscripts:

First subscript denoting the winding at which the cut is measured due to the current in the other winding, indicated by the second subscript. For example, L_{qd} is the mutual inductance between q and d axes windings due to a current in the d axis winding.

Under the predefined assumption of **uniform air gap**, the self-inductances are **independent** of angular positions which makes them **constants**.

$$L_{\alpha\alpha} = L_{\beta\beta} = L_{rr} \quad L_{dd} = L_{qq} = L_s. \quad (2.12)$$

The mutual inductances between stator and rotor windings are zero (0), as the flux set up by a current in one winding will not link with the other winding displaced in space by 90 degrees. This leads to the following simplifications.

$$L_{\alpha\beta} = L_{\beta\alpha} = 0$$

$$L_{dq} = L_{qd} = 0$$

The mutual inductances between the stator and rotor windings are a function of the rotor position, θ_r , and they are assumed to be sinusoidal functions based on our previous assumption of sinusoidal MMF distribution in the windings. Symmetry in windings and construction causes the mutual inductances between one stator and one rotor winding to be the same whether they are viewed from the stator or the rotor.

$$L_{\alpha d} = L_{d\alpha} = L_{sr} \cos \theta_r \quad (2.13)$$

$$L_{\beta d} = L_{d\beta} = L_{sr} \sin \theta_r \quad (2.14)$$

$$L_{\alpha q} = L_{q\alpha} = L_{sr} \sin \theta_r \quad (2.15)$$

$$L_{\beta q} = L_{q\beta} = -L_{sr} \cos \theta_r \quad (2.16)$$

where L_{sr} is the peak value of the mutual inductance between a stator and a rotor winding. The last equation has a negative term, because a positive current in β winding produces a negative flux linkage in the q axis winding, and vice versa. Substitution of equations from Eq. (2.12) to Eq. (2.13) into equations from Eq. (2.8) to Eq. (2.11) results in a system of differential equations with time-varying inductances. The resulting equations are as follows:

$$v_{qs} = (R_s + L_s p_t) i_{qs} + L_{sr} p_t (i_{\alpha} \sin \theta_r) - L_{sr} p_t (i_{\beta} \cos \theta_r) \quad (2.17)$$

$$v_{ds} = (R_s + L_s p_t) i_{ds} + L_{sr} p_t (i_{\alpha} \cos \theta_r) + L_{sr} p_t (i_{\beta} \sin \theta_r) \quad (2.18)$$

$$v_{\alpha} = L_{sr} p_t (i_{qs} \sin \theta_r) + L_{sr} p_t (i_{ds} \cos \theta_r) + (R_{rr} + L_{rr} p_t) i_{\alpha} \quad (2.19)$$

$$v_{\beta} = -L_{sr} p_t (i_{qs} \cos \theta_r) + L_{sr} p_t (i_{ds} \sin \theta_r) + (R_{rr} + L_{rr} p_t) i_{\beta} \quad (2.20)$$

where:

$$R_s = R_q = R_d \quad \text{and} \quad R_{rr} = R_{\alpha} = R_{\beta}$$

The solution of these equations is time-consuming, because of their dependence on the product of the instantaneous rotor-position-dependent cosine functions and winding currents, and an elegant set of equations leading to a simple solution procedure is necessary.

Transformations performing such a step are discussed subsequently.

2.4.2. Transformations for Constant Matrices

The transformation to obtain constant inductance values is achieved by replacing the actual with a fictitious rotor on the q and d axes as shown in Fig. 2.8.

In that process, the fictitious rotor will have the same number of turns for each phase as the actual rotor phase windings and should produce the same MMF. That leads to a calculation of the number

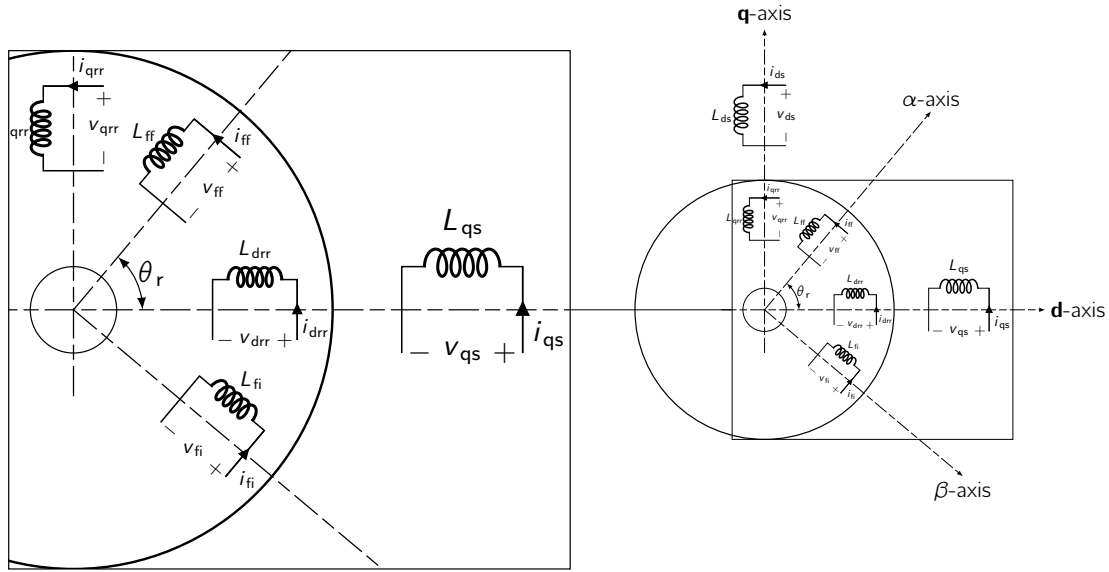


Figure 2.8.: Transformation on actual to fictitious rotor variables.

of turns on both sides of that equation, resulting in a relationship of the actual currents to fictitious rotor currents i_{qrr} and i_{drr} . Then the fictitious rotor currents i_{qrr} and i_{drr} are equal to the sum of the projections of i_α and i_β on the q and d axis, respectively, as given below:

$$\begin{bmatrix} i_{drr} \\ i_{qrr} \end{bmatrix} = \begin{bmatrix} \cos \theta_r & \sin \theta_r \\ \sin \theta_r & -\cos \theta_r \end{bmatrix} \begin{bmatrix} i_\alpha \\ i_\beta \end{bmatrix} \quad (2.21)$$

Eq. (2.21) is written compactly as:

$$\vec{i}_{dqrr} = [\mathbf{T}_{\alpha\beta}] \mathbf{i}_{\alpha\beta}$$

where

$$\vec{i}_{dqrr} = \begin{bmatrix} i_{drr} & i_{qrr} \end{bmatrix}^T \quad \text{and} \quad \mathbf{i}_{\alpha\beta} = \begin{bmatrix} i_\alpha & i_\beta \end{bmatrix}^T$$

and

$$\mathbf{T}_{\alpha\beta} = \begin{bmatrix} \cos \theta_r & \sin \theta_r \\ \sin \theta_r & -\cos \theta_r \end{bmatrix}$$

This transformation is valid for voltages, currents, and flux-linkages in a machine.

This transformation from α, β axes to d, q axes and vice versa is quite useful as:

$$\mathbf{T}_{\alpha\beta} = \mathbf{T}_{\alpha\beta}^{-1}$$

It is worth mentioning, that this matrix is both orthogonal and symmetric.

Applying this transformation to the α and β rotor-winding currents and rotor voltages in Eq. (2.19) and Eq. (2.20), the following matrix equation is obtained:

$$\begin{bmatrix} v_{qs} \\ v_{ds} \\ v_{qrr} \\ v_{drr} \end{bmatrix} = \begin{bmatrix} R_s + L_s p_t & 0 & L_s p_t & 0 \\ 0 & R_s + L_s p_t & 0 & L_{sr} p_t \\ L_s p_t & -L_s \dot{\theta}_r & R_{rr} + L_{rr} p_t & -L_{rr} \dot{\theta}_r \\ L_s \dot{\theta}_r & L_s p_t & L_{rr} \dot{\theta}_r & R_{rr} + L_{rr} p_t \end{bmatrix} \begin{bmatrix} i_{qs} \\ i_{ds} \\ i_{qrr} \\ i_{drr} \end{bmatrix}$$

where $\dot{\theta}_r$ is the time derivative of θ_r . The rotor equations need to be referred to the stator, as in the case of the transformer-equivalent circuit. This step removes the physical isolation and facilitates the corresponding stator and rotor **d** and **q** axes, windings in becoming physically connected. The steps involved in referring these rotor parameters and variables to the stator are as follows:

$$\begin{aligned} R_r &= a^2 R_{rr} & L_r &= a^2 L_{rr} & i_{qr} &= \frac{i_{qrr}}{a} \\ i_{dr} &= \frac{i_{drr}}{a} & v_{qr} &= a v_{qrr} & v_{dr} &= a v_{drr} \end{aligned}$$

where:

$$a = \frac{\text{Stator effective turns per phase}}{\text{Rotor effective turns per phase}} = \frac{k_{w1} T_1}{k_{w2} T_2} \quad (2.22)$$

Please be aware of the magnetising and mutual inductances as:

$$L_m \propto T_1^2 \quad L_{sr} \propto T_1 T_2 \quad (2.23)$$

From Eq. (2.22) and Eq. (2.23), the magnetising inductance of the stator as:

$$L_m = a L_{sr}$$

Using the aforementioned relations we can derive the machine equations referred to the stator as:

$$\begin{bmatrix} v_{qs} \\ v_{ds} \\ v_{qr} \\ v_{dr} \end{bmatrix} = \begin{bmatrix} R_s + L_s p_t & 0 & L_m p_t & 0 \\ 0 & R_s + L_s p_t & 0 & L_m p_t \\ L_m p_t & -L_m \dot{\theta}_r & R_r + L_r p_t & -L_r \dot{\theta}_r \\ L_m \dot{\theta}_r & L_m p_t & L_r \dot{\theta}_r & R_r + L_r p_t \end{bmatrix} \begin{bmatrix} i_{qs} \\ i_{ds} \\ i_{qr} \\ i_{dr} \end{bmatrix} \quad (2.24)$$

This equation is in the form where the voltage vector is equal to the product of the impedance matrix and current vector.

The impedance matrix has constant inductance terms and is no longer dependent on the rotor position.

Some of the impedance matrix elements are dependent on the rotor speed, and only when they are constant, as in steady state, does the system of equations become linear. In the case of varying rotor speed and if its variation is dependent on the currents, then the system of equations becomes non-linear. It is derived later that the electromagnetic torque, as a function of winding currents and rotor speed, is determined by the electromagnetic and load torques along with load parameters such as inertia and friction. In that case, it can be seen that the induction-machine system is non-linear.

2.4.3. Three-Phase to Two-Phase Transformation

We have now a model for a **two-phase IM**, however compared to a 3-phase it is seldom used. Therefore we need to be able to create a bridge between 2-phase and 3-phase model. For this, we need to establish an **equivalence**. This equivalence is based on the equality of the MMF produced in the two-phase and three-phase windings and equal current magnitudes.

Assuming each of the three-phase windings has T_1 turns per phase and equal current magnitudes, the two-phase windings will have $3T_1/2$ turns per phase for MMF equality. The **d** and **q** axes MMFs are found by resolving the MMFs of the three phases along the **d** and **q** axes.

The common term, the number of turns in the winding, is cancelled on either side of the equations, leaving the current equality.

The **q** axis is assumed to be lagging the **a** axis by θ_c . The relationship between **dq0** and **abc** currents is as follows:

$$\begin{bmatrix} i_{qs} \\ i_{ds} \\ i_0 \end{bmatrix} = \frac{2}{3} \begin{bmatrix} \cos \theta_c & \cos \left(\theta_c - 2\frac{\pi}{3} \right) & \cos \left(\theta_c + 2\frac{\pi}{3} \right) \\ \sin \theta_c & \sin \left(\theta_c - 2\frac{\pi}{3} \right) & \sin \left(\theta_c + 2\frac{\pi}{3} \right) \\ \frac{1}{2} & \frac{1}{2} & \frac{1}{2} \end{bmatrix} \begin{bmatrix} i_{as} \\ i_{bs} \\ i_{cs} \end{bmatrix} \quad (2.25)$$

The current i_0 , represents the **imbalances** in the *a*, *b*, and *c* phase currents and can be recognised as the zero-sequence component of the current. Eq. (2.23) can be expressed in a compact form by

$$\vec{i}_{qd0} = \vec{T}_{abc} \vec{i}_{abc}$$

where

$$\vec{i}_{qd0} = [i_{qs} \quad i_{ds} \quad i_0]^T \quad \vec{i}_{abc} = [i_{as} \quad i_{bs} \quad i_{cs}]^T$$

and the transformation from **abc** to **qdo** variables is [35]:

$$\vec{T}_{abc} = \frac{2}{3} \begin{bmatrix} \cos \theta_c & \cos \left(\theta_c - 2\frac{\pi}{3} \right) & \cos \left(\theta_c + 2\frac{\pi}{3} \right) \\ \sin \theta_c & \sin \left(\theta_c - 2\frac{\pi}{3} \right) & \sin \left(\theta_c + 2\frac{\pi}{3} \right) \\ \frac{1}{2} & \frac{1}{2} & \frac{1}{2} \end{bmatrix} \quad (2.26)$$

The zero-sequence current, i_0 , does not produce a resultant magnetic field.

The transformation from two-phase currents to three-phase currents can be obtained as:

$$\vec{i}_{abc} = \vec{T}_{abc}^{-1} \vec{i}_{qd0}$$

This transformation could also be thought of as a transformation from three (3) (**abc**) axes to three new (**qdo**) axes; for uniqueness of the transformation from one set of axes to another set of axes, including unbalanced in the **abc** variables requires three (3) variables:

... such as the **dq0**.

The reason for this is that it is easy to interpret from the **abc** variables to **qd** variables if the **abc** variables have an inherent relationship among the two (2) variables as the equal-phase idea here and magnitude. Therefore, in such a case, there are only two independent variables in **abc** with the third being a dependent variable, obtained as the negative sum of the other two variables.

Therefore a **dq0-to-abc** transformation is unique under the aforementioned circumstance. When the **abc** variables have no such inherent relationship, then there are three distinct and independent variables; hence, the third variable cannot be recovered from the knowledge of the other two variables only. It also means that they are not recoverable from two (2) variables **qd** but require another variable, such as the zero-sequence component, to recover the **abc** variables from the **dq0** variables.

Under balanced conditions only, there are four (4) system equations, as given in Eq. (2.24). Under unbalanced conditions, note that two (2) more system equations, one for the stator zero-sequence voltage and the other for the rotor zero-sequence voltage, emerge. They are given as:

$$v_{os} = R_s + L_{ls} p_t i_{os} \quad v_{or} = R_r + L_{lr} p_t i_{or}$$

where in the variables the first subscript (*o*) denotes the **zero-sequence component** and the second subscript denotes the stator and rotor by *s* and *r*, respectively. They could be derived from the stator and rotor inductance matrices in the **abc** frames, then converted into **dq0** frames by using the transformation derived above.

It is interesting to observe that only leakage inductances and phase resistances influence the zero-sequence voltages and currents, unlike in the **dq** component variables, which are influenced by the self and mutual inductances and phase resistances.

It is usual to align the **q** axis with the phase *a* winding; this implies that the **qd** frames are fixed to the stator²⁵. In that case, $\theta_c = 0$, and the transformation from **abc** to **qd0** variables is given as

$$T_{abc}^s = \frac{2}{3} \begin{bmatrix} 1 & -\frac{1}{2} & -\frac{1}{2} \\ 0 & -\frac{\sqrt{3}}{2} & \frac{\sqrt{3}}{2} \\ \frac{1}{2} & \frac{1}{2} & \frac{1}{2} \end{bmatrix} \quad (2.27)$$

In a balanced three-phase machine, the sum of the three-phase currents is zero and is given as

$$i_{as} + i_{bs} + i_{cs} = 0$$

leading to a zero-sequence current of zero value:

$$i_0 = \frac{1}{3} (i_{as} + i_{bs} + i_{cs}) = 0 \quad (2.28)$$

With Eq. (??), the equivalence²⁶ between the two-phase and three-phase IMs is established.

²⁵The model is known as Stanley's model or the stator reference frames model [36].

²⁶It is instructive to know that the transformation derived is applicable to currents, voltages, and flux-linkages.

Exercise 2.1: Calculating d-q currents

An IM has the following parameters:

$$\begin{array}{llll} 5 \text{ hp} & 3\text{-phase} & 4\text{-pole} & \text{star-connected} \\ R_s = 0.277 \text{ } \Omega & R_r = 0.183 \text{ } \Omega & L_m = 0.0538 \text{ H} & L_s = 0.0533 \text{ H} \\ L_r = 0.056 \text{ H} & a = 3 & & \end{array}$$

where a is the effective stator to rotor turns ratio. The motor is supplied with its rated and balanced voltages. Find the q , d axes steady-state voltages and currents when the rotor is locked. Use the stator-reference-frame model of the IM.

Solution

The applied phase voltages are as follows:

$$\begin{aligned} v_{as} &= \frac{200}{\sqrt{3}} \times \sqrt{2} \sin \omega_s t = 163.3 \sin \omega_s t \\ v_{bs} &= 163.3 \sin \left(\omega_s t - \frac{2\pi}{3} \right) \\ v_{cs} &= 163.3 \sin \left(\omega_s t + \frac{2\pi}{3} \right) \end{aligned}$$

The d and q axes voltages are

$$\begin{bmatrix} v_{qs} \\ v_{ds} \\ v_0 \end{bmatrix} = \tilde{T}_{abc}^s \begin{bmatrix} v_{as} \\ v_{bs} \\ v_{cs} \end{bmatrix}$$

Therefore,

$$v_{qs} = \frac{2}{3} \left[v_{as} - \frac{1}{2} (v_{bs} + v_{cs}) \right]$$

For a balanced three-phase input:

$$v_{as} + v_{bs} + v_{cs} = 0$$

Substituting for v_{bs} and v_{cs} in terms of v_{as} gives

$$v_{qs} = \frac{2}{3} \left[\frac{3}{2} v_{as} \right] = v_{as}$$

Similarly,

$$v_{ds} = \frac{1}{\sqrt{3}} (v_{cs} - v_{bs})$$

and $v_0 = 0$

$$v_{qs} = v_{as} = 163.3 \sin \omega_s t = 163.3 \angle 0^\circ = 163.3 \text{ V}$$

$$v_{ds} = \frac{1}{\sqrt{3}} (v_{cs} - v_{bs}) = 163.3 \cos \omega_s t = 163.3 \angle 90^\circ = j 163.3 \text{ V}$$

The rotor is locked, therefore:

$$\dot{\theta}_r = 0$$

For steady-state evaluation:

$$p_t = j \omega_s = j 2\pi f_s = j 2\pi 60 = j 377 \text{ rad s}^{-1}$$

The system equations are:

$$\begin{bmatrix} v_{qs} \\ v_{ds} \\ 0 \\ 0 \end{bmatrix} = \begin{bmatrix} R_s + j \omega_s L_s & 0 & j \omega_s L_m & 0 \\ 0 & R_s + j \omega_s L_s & 0 & j \omega_s L_m \\ j \omega_s L_m & 0 & R_r + j \omega_s L_r & 0 \\ 0 & j \omega_s L_m & 0 & R_r + j \omega_s L_r \end{bmatrix} \begin{bmatrix} i_{qs} \\ i_{ds} \\ i_{qr} \\ i_{dr} \end{bmatrix} \quad (2.29)$$

Note that the rotor windings are **short-circuited**, and hence rotor voltages are zero. The numerical values for the parameters and variables are substituted to solve for the currents. The currents are

$$i_{qs} = 35.37 - j 108.18 = 113.81 \angle -71.90^\circ$$

$$i_{ds} = 108.18 + j 35.37 = 113.81 \angle 18.90^\circ$$

$$i_{qr} = -34.88 + j 103.63 = 109.34 \angle 108.60^\circ$$

$$i_{dr} = -103.63 - j 34.88 = 109.34 \angle -161.40^\circ$$

Note that the stator and rotor currents are displaced by 90° among themselves, as expected in a two-phase machine. The zero-sequence currents are zero because zero-sequence voltages are non-existent with balanced supply voltages ■.

2.4.4. Power Equivalence

The power input to the three-phase motor must be equal to the power input to the two-phase machine for it to have a meaningful interpretation in the modelling, analysis, and simulation.

The three-phase **instantaneous power input** is:

$$p_i = \vec{v}_{abc}^t \vec{i}_{abc} = v_{as}i_{as} + v_{bs}i_{bs} + v_{cs}i_{cs} \quad (2.30)$$

From Eq. (2.25), the **abc** phase currents and voltages are transformed into their equivalent **qd** currents and voltages as:

$$\vec{i}_{abc} = [\vec{T}_{abc}]^{-1} \vec{i}_{qd0} \quad \text{and} \quad \vec{v}_{abc} = [\vec{T}_{abc}]^{-1} \vec{v}_{qd0} \quad (2.31)$$

Substituting Eq. (2.31) into Eq. (2.30) gives the power input as:

$$p_i = \vec{v}_{qd0}^t \left([\vec{T}_{abc}]^{-1} \right)^t [\vec{T}_{abc}]^{-1} \vec{i}_{qd0}. \quad (2.32)$$

Expanding the Right Hand Side (RHS) of Eq. (2.32) gives the power input in **dq0** variables:

$$p_i = \frac{3}{2} \left((v_{qs}i_{qs} + v_{ds}i_{ds}) + 2v_0i_0 \right) \quad (2.33)$$

For a **balanced three-phase machine**, the zero-sequence current does not exist. Therefore, the power input is compactly represented by

$$p_i = \frac{3}{2} (v_{qs}i_{qs} + v_{ds}i_{ds}) \quad (2.34)$$

The model we have development thus far kept the **dq** axes **stationary with respect to the stator**. These axes or frames are known as reference frames.

The input power given by Eq. (2.33) remains valid for all occasions, provided that the voltages and currents correspond to the frames under consideration.

2.4.5. Generalised Model in Arbitrary Reference Frame

Reference frames are very much like observer platforms, in that each of the platform gives a unique view of the system at hand as well as a dramatic simplification of the system equations.

For the purposes of control, it is desirable to have the system variables as DC quantities, although the actual variables are sinusoidal.

This could be accomplished by having a reference frame revolving at the same angular speed as that of the sinusoidal variable. As the reference frames are moving at an angular speed equal to the

angular frequency of the sinusoidal supply, say, then the differential speed between them is reduced to zero, resulting in the sinusoidal being perceived as a DC signal from the reference frames. Then, by moving to that plane, it becomes easier to develop a small-signal equation out of a non-linear equation, as the operation is described only by DC values. This then leads to the linearised system around an operating point. Now, it is easier to create a compensator for the system by using standard linear control-system techniques.

the independent rotor-field position determines the induced EMF and affects the dynamic system equations of both the wound-rotor and Permanent Magnet Synchronous Motor (PMSM).

Therefore, looking at the entire system from the rotor²⁷, the system inductance matrix becomes independent of rotor position, therefore leading to the simplification and compactness of the system equations. Such advantages are many from using reference frames. Instead of deriving the transformations for each and every particular reference frame, it is advantageous to derive the general transformation for an arbitrary rotating reference frame. Then any particular reference frame model can be derived by substituting the appropriate frame speed and position in the generalised reference model.

²⁷ rotating reference frames applied

Reference frames rotating at an arbitrary speed are hereafter called arbitrary reference frames. Other reference frames are particular cases of these arbitrary reference frames. From now on, the three-phase machine is assumed to have balanced windings and balanced inputs, thus making the zero-sequence components be zero (0) and eliminating the zero-sequence equations from further consideration.

the zero-sequence equations have to be included only for unbalanced operation of the motor, a situation common with a fault in the machine²⁸ or converter.

²⁸ which could be a very interesting M.Sc thesis topic

Assuming the windings have equal number of turns on both of the reference frames, the arbitrary reference frame currents are resolved on the **d, q** axes to find the currents in the stationary reference frames. The relationships between the currents are written as:

$$i_{qds} = [T^c] i_{qds}^c$$

where:

$$i_{qds} = \begin{bmatrix} i_{qs} & i_{ds} \end{bmatrix}^T \quad i_{qds}^c = \begin{bmatrix} i_{qs}^c & i_{ds}^c \end{bmatrix}^T$$

and:

$$T^c = \begin{bmatrix} \cos \theta_c & \sin \theta_c \\ -\sin \theta_c & \cos \theta_c \end{bmatrix}$$

The speed of the arbitrary reference frames is:

$$\dot{\theta}_c = \omega_c$$

Similarly, the fictitious rotor currents are transformed into arbitrary frames by using T^c , and they are written as

$$i_{qdr} = [T^c] i_{qdr}^c$$

where:

$$i_{qdr} = \begin{bmatrix} i_{qr} & i_{dr} \end{bmatrix}^T \quad i_{qdr}^c = \begin{bmatrix} i_{qr}^c & i_{dr}^c \end{bmatrix}^T$$

And similarly, the voltage relationships are:

$$v_{qds} = [T^c] v_{qds}^c \quad v_{qdr} = [T^c] v_{qdr}^c$$

where, as usual:

$$\begin{aligned} v_{qds} &= \begin{bmatrix} v_{qs} & v_{ds} \end{bmatrix}^T & v_{qds}^c &= \begin{bmatrix} v_{qs}^c & v_{ds}^c \end{bmatrix}^T \\ v_{qdr} &= \begin{bmatrix} v_{qr} & v_{dr} \end{bmatrix}^T & v_{qdr}^c &= \begin{bmatrix} v_{qr}^c & v_{dr}^c \end{bmatrix}^T \end{aligned}$$

By substituting the aforementioned equations into Eq. (2.24), the IM in arbitrary reference frame is obtained which is shown as:

$$\begin{bmatrix} v_{qs}^c \\ v_{ds}^c \\ v_{qr}^c \\ v_{dr}^c \end{bmatrix} = \begin{bmatrix} R_s + L_s p_t & \omega_c L_s & L_m p_t & \omega_c L_m \\ -\omega_c L_s & R_s + L_s p_t & -\omega_c L_m & L_m p_t \\ L_m p_t & (\omega_c - \omega_r) L_m & R_r + L_r p_t & (\omega_c - \omega_r) L_r \\ -(\omega_c - \omega_r) L_m & L_m p_t & -(\omega_c - \omega_r) L_r & R_r + L_r p_t \end{bmatrix} \begin{bmatrix} i_{qs}^c \\ i_{ds}^c \\ i_{qr}^c \\ i_{dr}^c \end{bmatrix} \quad (2.35)$$

where:

$$\omega_r = \dot{\theta}_r$$

ω_r is the rotor speed in electrical rpm. The relationship between the arbitrary reference frame variables and the a , b , and c variables is derived by using

$$i_{qds}^c = [T^c]^{-1} i_{qds}$$

By substituting from Eq. (2.27) for i_{qds} in terms of a , b , and c phase currents in the stator reference frames, the **qd0** currents in the arbitrary reference frames are obtained as:

$$i_{qd0}^c = \begin{bmatrix} [T^c]^{-1} & 0 \\ [0] & 1 \end{bmatrix} [T_{abc}^s] [i_{abc}] = [T_{abc}] [i_{abc}]$$

where $[0]$ is a 1×2 null vector. Note that the zero-sequence currents remain unchanged in the arbitrary reference frames. This transformation is valid for currents, voltages, and flux-linkages for both the stator and the rotor. Particular cases of the reference frames are derived in a later section. The next section contains the derivation of the electromagnetic torque in terms of the current variables in the arbitrary reference frames.

2.4.6. Electromagnetic Torque

The electromagnetic torque (T_e) is an important output variable which determines such mechanical dynamics of the machine as the rotor position and speed. Therefore, its importance cannot be overstated in any of the simulation studies. It is derived from the machine matrix equation by looking at the input power and its various components, such as:

resistive losses, mechanical power, rate of change of stored magnetic energy, and reference-frame power [37]

Elementary reasoning leads to the fact that there cannot be a power component due to the introduction of reference frames. Similarly, the rate of change of stored magnetic energy must be zero in steady state. Hence, the output power is the difference between the input power and the resistive losses in steady state. Dynamically, the rate of change of stored magnetic energy need **NOT** be zero (0) .

Based on these observations, the derivation of the electromagnetic torque is made as follows. The equation (5.114) can be written as

$$\vec{V} = \vec{R}\vec{i} + \vec{L}\dot{\vec{p}}_t\vec{i} + \vec{G}\omega_r\vec{i} + \vec{F}\omega_c\vec{i},$$

where the vectors and matrices are identified by observation. Pre-multiplying the equation Eq. (2.4.6) by the transpose of the current vector (\vec{i}^T) gives the instantaneous input power as,

$$\bar{p}_i = \vec{i}^T \vec{V} = \vec{i}^T \vec{R}\vec{i} + \vec{i}^T \vec{L}\dot{\vec{p}}_t\vec{i} + \vec{i}^T \vec{G}\omega_r\vec{i} + \vec{i}^T \vec{F}\omega_c\vec{i}$$

where:

\vec{R} consists of resistive elements,

\vec{L} consists of the coefficients of the derivative operator $\dot{\vec{p}}_t$,

\vec{G} elements that are the coefficients of the electrical rotor speed ω_r ,

\vec{F} frame matrix in terms of the coefficients of the reference frame speed, ω_c

$\vec{i}^T \vec{R}\vec{i}$ Stator and rotor resistive losses.

$\vec{i}^T \vec{F}\omega_c\vec{i}$ The reference frame power, ²⁹

$\vec{i}^T \vec{L}\dot{\vec{p}}_t\vec{i}$ The rate of change of stored magnetic energy.

Therefore, what is left of the power component must be equal to the air gap power, given by the term $\vec{i}^T \vec{G}\omega_r\vec{i}$. From fundamentals, it is known the air gap power has to be associated with the rotor speed.

²⁹ upon expansion is found to be identically equal to zero, as it should be, because there cannot be a power associated with a fictitious element introduced for the sake of simplifying the model and analysis.

The air gap power is the product of the mechanical rotor speed and air gap or electromagnetic torque.

Therefore the air-gap torque, T_e , is derived from the terms involving the rotor speed, ω_m in mechanical rad s^{-1} , as

$$\omega_m T_e = P_{\text{air-gap}} = \vec{i}^T \vec{G}\vec{i} \times \omega_r$$

Substituting for ω_r in terms of ω_m leads to electromagnetic torque as

$$T_e = \frac{\vec{P}}{2} \vec{i}^t \vec{G} \vec{i} \quad (2.36)$$

By substituting for \vec{G} in equation Eq. (2.36) by observation from Eq. (2.35), the electromagnetic torque is obtained as:

$$\vec{T}_e = \frac{3}{2} \frac{\vec{P}}{2} L_m \left(i_{qs}^c i_{dr}^c - i_{ds}^c i_{qr}^c \right) \quad (2.37)$$

The factor $3/2$ is introduced into the right-hand side of equation Eq. (2.37) from the power-equivalence condition between the three-phase and two-phase IMs. The next section considers the frequently used models in various reference frames and their derivation from the generalised induction-motor model in arbitrary reference frames.

2.4.7. Derivation of Commonly Used Induction-Machine Models

There are three (3) particular cases of the generalised model of the IM in arbitrary reference frames are of general interest:

1. stator reference frames model;
2. rotor reference frames model;
3. synchronously rotating reference frames model.

Let's look at each of them in more detail.

Stator Reference

The speed of the reference frames is that of the stator, which is zero.

$$\omega_c = 0 \quad (2.38)$$

This is substituted to Eq. (2.35) to derive the following model:

$$\begin{bmatrix} v_{qs} \\ v_{ds} \\ v_{qr} \\ v_{dr} \end{bmatrix} = \begin{bmatrix} R_s + L_s p_t & 0 & L_m p_t & 0 \\ 0 & R_s + L_s p_t & 0 & L_m p_t \\ L_m p_t & -\omega_r L_m & R_r + L_r p_t & -\omega_r L_r \\ \omega_r L_m & L_m p_t & \omega_r L_r & R_r + L_r p_t \end{bmatrix} \begin{bmatrix} i_{qs} \\ i_{ds} \\ i_{qr} \\ i_{dr} \end{bmatrix} \quad (2.39)$$

For convenience, the superscript is omitted for the stator reference frames model hereafter.

The torque equation is

$$\vec{T}_e = \frac{3}{2} \frac{\bar{P}}{2} L_m (i_{qs} i_{dr} - i_{ds} i_{qr}) \quad (2.40)$$

Note that Eq. (2.39) and Eq. (2.24) are identical. The transformation for variables is obtained by substituting $\theta_c = 0$ in $[T_{abc}]$ and will be the same as $[T_{abc}^S]$, defined in Eq. (2.27).

This model is used when stator variables are required to be actual³⁰, and rotor variables can be fictitious. This model allows simple simulation of stator-controlled IM drives, such as phase-controlled and inverter-controlled induction-motor drives, as the input variables are well defined and could be used to find the stator **qd** axes voltages through a set of simple algebraic equations, for a **balanced** poly-phase supply input, given by:

³⁰i.e., the same as in the actual machine stator

$$v_{qs} = v_{as} \quad \text{and} \quad v_{ds} = \frac{(v_{cs} - v_{bs})}{\sqrt{3}}$$

These algebraic relationships reduce the number of computations and therefore lend themselves to real-time control applications in high-performance variable-speed drives requiring the computation of stator currents, stator flux linkages, and electromagnetic torque for both control and parameter adaptation.

Rotor Reference

The speed of the rotor reference frame is:

$$\omega_c = \omega_r \quad (2.41)$$

and the angular position is:

$$\theta_c = \theta_r \quad (2.42)$$

Substituting in the upper subscript r for rotor reference frames and Eq. (2.41) in Eq. (2.35), the induction-motor model in rotor reference frames is obtained. The equations are given by

$$\begin{bmatrix} v_{qs}^r \\ v_{ds}^r \\ v_{qr}^r \\ v_{dr}^r \end{bmatrix} = \begin{bmatrix} R_s + L_s p_t & \omega_r L_s & L_m p_t & \omega_r L_m \\ -\omega_r L_s & R_s + L_s p_t & -\omega_r L_m & L_m p_t \\ L_m p_t & 0 & R_r + L_r p_t & -0 \\ 0 & L_m p_t & 0 & R_r + L_r p_t \end{bmatrix} \begin{bmatrix} i_{qs}^r \\ i_{ds}^r \\ i_{qr}^r \\ i_{dr}^r \end{bmatrix} \quad (2.43)$$

The torque equation is

$$\vec{T}_e = \frac{3}{2} \frac{P}{2} L_m (i_{qs}^r i_{dr}^r - i_{ds}^r i_{qr}^r) \quad (2.44)$$

The transformation from **abc** to **dq0** variables is obtained by substituting Eq. (2.42) to $[T_{abc}]$,

defined in Eq. (2.26) as:

$$[T_{abc}^r] = \frac{2}{3} \begin{bmatrix} \cos \theta_r & \cos(\theta_r - 2\frac{\pi}{3}) & \cos(\theta_r + 2\frac{\pi}{3}) \\ \sin \theta_r & \sin(\theta_r - 2\frac{\pi}{3}) & \sin(\theta_r + 2\frac{\pi}{3}) \\ \frac{1}{2} & \frac{1}{2} & \frac{1}{2} \end{bmatrix} \quad (2.45)$$

The rotor reference frames model is useful where the switching elements and power are controlled on the rotor side. Slip-power recovery scheme is one example where this model will find use in the simulation of the motor-drive system.

Synchronous Rotation Reference

The reference frames is

$$\omega_c = \omega_s = \text{Stator supply angular frequency} \quad (2.46)$$

and the instantaneous angular position is

$$\theta_c = \theta_s = \omega_s t \quad (2.47)$$

By substituting Eq. (2.47) into Eq. (2.35), the induction-motor model in the synchronous reference frames is obtained. By using the superscript e to denote this electrical synchronous reference frame, the model is obtained as

$$\begin{bmatrix} v_{qs}^e \\ v_{ds}^e \\ v_{qr}^e \\ v_{dr}^e \end{bmatrix} = \begin{bmatrix} R_s + L_s p_t & \omega_s L_s & L_m p_t & \omega_s L_m \\ -\omega_s L_s & R_s + L_s p_t & -\omega_s L_m & L_m p_t \\ L_m p_t & (\omega_s - \omega_r) L_m & R_r + L_r p_t & (\omega_s - \omega_r) L_r \\ -(\omega_s - \omega_r) L_m & L_m p_t & -(\omega_s - \omega_r) L_r & R_r + L_r p_t \end{bmatrix} \begin{bmatrix} i_{qs}^e \\ i_{ds}^e \\ i_{qr}^e \\ i_{dr}^e \end{bmatrix} \quad (2.48)$$

The torque equation is

$$\vec{T}_e = \frac{3}{2} \frac{P}{2} L_m (i_{qs}^e i_{dr}^e - i_{ds}^e i_{qr}^e) \quad \text{N m} \quad (2.49)$$

The transformation from abc to dqo variables is found by substituting Eq. (2.47) into Eq. (2.26) and is given as:

$$[T_{abc}^e] = \frac{2}{3} \begin{bmatrix} \cos \theta_e & \cos(\theta_e - 2\frac{\pi}{3}) & \cos(\theta_e + 2\frac{\pi}{3}) \\ \sin \theta_e & \sin(\theta_e - 2\frac{\pi}{3}) & \sin(\theta_e + 2\frac{\pi}{3}) \\ \frac{1}{2} & \frac{1}{2} & \frac{1}{2} \end{bmatrix} \quad (2.50)$$

It may be seen that the synchronous reference frames transform the sinusoidal inputs into DC signals. This model is useful where the variables in steady state need to be DC quantities, as in the development of small-signal equations. Some high-performance control schemes use this model to estimate the control inputs.

This led to a major breakthrough in induction-motor control, by decoupling the torque and flux channels for control in a manner similar to that for separately-excited DC motor drives. This is dealt with in detail on vector control schemes on the next chapter.

2.4.8. Equations in Flux Linkages

The dynamic equations of the IM in **arbitrary reference** frames can be represented by using flux linkages as variables. This involves the reduction of a number of variables in the dynamic equations.

Even when the voltages and currents are discontinuous, the flux linkages are continuous.

This gives the advantage of differentiating these variables with numerical stability. In addition, the flux-linkages representation is used in motor drives to highlight the process of the decoupling of the flux and torque channels in the induction and synchronous machines.

The stator and rotor flux linkages in the arbitrary reference frames are defined as

$$\lambda_{qs}^c = L_s i_{qs}^c + L_m i_{qr}^c, \lambda_{ds}^c = L_s i_{ds}^c + L_m i_{dr}^c, \lambda_{qr}^c = L_r i_{qr}^c + L_m i_{qs}^c, \lambda_{dr}^c = L_r i_{dr}^c + L_m i_{ds}^c \quad (2.51)$$

The zero-sequence flux linkages are

$$\lambda_{os} = L_{ls} i_{os}, \quad \lambda_{or} = L_{lr} i_{or}.$$

The **q** axis stator voltage in the arbitrary reference frame is

$$v_{qs}^c = R_s i_{qs}^c + \omega_c (L_s i_{ds}^c + L_m i_{dr}^c) + L_m p_t i_{qr}^c + L_s p_t i_{qs}^c$$

Substituting from the defined flux-linkages into the voltage equation gives:

$$v_{qs}^c = R_s i_{qs}^c + \omega_c \lambda_{ds}^c + p_t \lambda_{qs}^c \quad (2.52)$$

Similarly, the stator **d** axis voltage, the **dq**-axes rotor voltages, and the zero-sequence voltage equations are derived as:

$$v_{ds}^c = R_s i_{ds}^c - \omega_c \lambda_{qs}^c + p_t \lambda_{ds}^c \quad (2.53)$$

$$v_{os} = R_s i_{os} + p_t \lambda_{os} \quad (2.54)$$

$$v_{qr}^c = R_r i_{qr}^c + (\omega_c - \omega_r) \lambda_{dr}^c + p_t \lambda_{qr}^c \quad (2.55)$$

$$v_{dr}^c = R_r i_{dr}^c - (\omega_c - \omega_r) \lambda_{qr}^c + p_t \lambda_{dr}^c \quad (2.56)$$

$$v_{or} = R_r i_{or} + p_t \lambda_{or} \quad (2.57)$$

To simplify these expression we can represent them as per-unit values. The normalisation of the variables is made via reactances rather than inductances. To facilitate such a step, a modified flux linkage is defined whose unit in volts is

$$\Psi_{qs}^c = \omega_b \lambda_{qs}^c = \omega_b (L_s i_{qs}^c + L_m i_{qr}^c) = X_s i_{qs}^c + X_m i_{qr}^c$$

where ω_b is the base frequency in rad s^{-1} . The other modified flux linkages can be written as:

$$\Psi_{ds}^c = X_s i_{ds}^c + X_m i_{dr}^c$$

$$\Psi_{qs}^c = X_s i_{qr}^c + X_m i_{qs}^c$$

$$\Psi_{ds}^c = X_r i_{dr}^c + X_m i_{ds}^c$$

$$\Psi_{os} = X_{ls} i_{os}$$

$$\Psi_{or} = X_{lr} i_{or}$$

Substituting the flux linkages in terms of the modified flux linkages gives:

$$\lambda_{qs}^c = \frac{\Psi_{qs}^c}{\omega_b}, \lambda_{ds}^c = \frac{\Psi_{ds}^c}{\omega_b}, \lambda_{os}^c = \frac{\Psi_{os}^c}{\omega_b}, \lambda_{qr}^c = \frac{\Psi_{qr}^c}{\omega_b}, \lambda_{dr}^c = \frac{\Psi_{dr}^c}{\omega_b}, \lambda_{or}^c = \frac{\Psi_{or}^c}{\omega_b} \quad (2.58)$$

and by substituting equation Eq. (2.58) into equations from Eq. (2.52) to Eq. (2.57), the resulting equations in the modified flux linkages are:

$$\begin{aligned} v_{qs}^c &= R_s i_{qs}^c + \frac{\omega_c}{\omega_b} \Psi_{ds}^c + \frac{p_t}{\omega_b} \Psi_{qs}^c \\ v_{ds}^c &= R_s i_{ds}^c - \frac{\omega_c}{\omega_b} \Psi_{qs}^c + \frac{p_t}{\omega_b} \Psi_{ds}^c \\ v_{os} &= R_s i_{os} + \frac{p_t}{\omega_b} \Psi_{os} \\ v_{qr}^c &= R_r i_{qr}^c + \frac{(\omega_c - \omega_r)}{\omega_b} \Psi_{dr}^c + \frac{p_t}{\omega_b} \Psi_{qr}^c \\ v_{dr}^c &= R_r i_{dr}^c - \frac{(\omega_c - \omega_r)}{\omega_b} \Psi_{qr}^c + \frac{p_t}{\omega_b} \Psi_{dr}^c \\ v_{or} &= R_r i_{or} + \frac{p_t}{\omega_b} \Psi_{or} \end{aligned}$$

The electromagnetic torque in flux linkages and currents is derived as:

$$T_e = \frac{3}{2} \frac{P}{2} L_m \left(i_{qs}^c i_{dr}^c - i_{ds}^c i_{qs}^c \right) = \frac{3}{2} \frac{P}{2} \left(i_{qs}^c (L_m i_{dr}^c) - i_{ds}^c (L_m i_{qr}^c) \right)$$

The rotor current can be substituted in terms of the stator currents and stator flux linkages from the basic definitions of the flux linkages. From Eq. (2.51):

$$L_m i_{dr}^c + L_s i_{ds}^c = \lambda_{ds}^c \quad (2.59)$$

Which makes

$$L_m i_{dr}^c = (\lambda_{ds}^c - L_s i_{ds}^c) \quad \text{and} \quad L_m i_{qr}^c = (\lambda_{qs}^c - L_s i_{qs}^c) \quad (2.60)$$

Substituting Eq. (2.59) and Eq. (2.60) to X gives the electromagnetic torque in stator flux linkages and stator currents as:

$$T_e = \frac{3}{2} \frac{P}{2} \left(i_{qs}^c (\lambda_{ds}^c - L_s i_{ds}^c) - i_{ds}^c (\lambda_{qs}^c - L_s i_{qs}^c) \right) = \frac{3}{2} \frac{P}{2} \left(i_{qs}^c \lambda_{ds}^c - i_{ds}^c \lambda_{qs}^c \right)$$

Or we can write electromagnetic torque in terms of modified flux linkages and currents as:

$$T_e = \frac{3}{2} \frac{P}{2} \frac{1}{\omega_b} \left(i_{qs}^c \Psi_{ds}^c - i_{ds}^c \Psi_{qs}^c \right)$$

The electromagnetic torque can also be expressed using only rotor variables which has been left to the reader as exercise.

2.5. Dynamic Simulation Equations

The dynamic simulation of the IM is explained in this section. The equations of the IM in arbitrary reference frames in p.u. are cast in the state-space form as:

$$\vec{P}_1 p_t \vec{X}_1 + \vec{Q}_1 \vec{X}_1 = u_1$$

where

$$\vec{P} = \begin{bmatrix} \frac{X_{sn}}{\omega_b} & 0 & \frac{X_{mn}}{\omega_b} & 0 \\ 0 & \frac{X_{sn}}{\omega_b} & 0 & \frac{X_{mn}}{\omega_b} \\ \frac{X_{mn}}{\omega_b} & 0 & \frac{X_{rn}}{\omega_b} & 0 \\ 0 & \frac{X_{mn}}{\omega_b} & 0 & \frac{X_{rn}}{\omega_b} \end{bmatrix} \quad \vec{X} = \begin{bmatrix} i_{qsn}^c \\ i_{dsn}^c \\ i_{qrn}^c \\ i_{drn}^c \end{bmatrix} \quad \vec{U} = \begin{bmatrix} V_{qsn}^c \\ V_{dsn}^c \\ V_{qrn}^c \\ V_{drn}^c \end{bmatrix}$$

$$\vec{Q} = \begin{bmatrix} R_{sn} & \omega_{cn} X_{sn} & 0 & \omega_{cn} X_{mn} \\ -\omega_{cn} X_{sn} & R_{sn} & -\omega_{cn} X_{mn} & 0 \\ 0 & (\omega_{cn} - \omega_{rn}) X_{mn} & R_{rn} & (\omega_{cn} - \omega_{rn}) X_{mn} \\ -(\omega_{cn} - \omega_{rn}) X_{mn} & 0 & -(\omega_{cn} - \omega_{rn}) X_{rn} & R_{rn} \end{bmatrix}$$

The equations can be re-arranged in the state-space form as:

$$p_t \vec{X} = \vec{P}^{-1} (\vec{U} - \vec{Q} \vec{X})$$

Which can be re-written as:

$$p_t \vec{X} = \vec{A} \vec{X} + \vec{B} \vec{U} \quad \text{where} \quad \vec{A} = -\vec{P}^{-1} \vec{Q} \quad \text{and} \quad \vec{B} = \vec{P}^{-1}$$

These aforementioned expressions are evaluated to be:

$$\vec{B} = \vec{P}^{-1} = \frac{1}{\Delta} \begin{bmatrix} X_{rn} & 0 & -X_{mn} & 0 \\ 0 & X_{rn} & 0 & -X_{mn} \\ -X_{mn} & 0 & X_{sn} & 0 \\ 0 & -X_{mn} & 0 & X_{sn} \end{bmatrix} \quad \text{where} \quad \Delta = \left(\frac{X_{sn} X_{rn} - X_{mn}^2}{\omega_b} \right)$$

and let's not forget the matrix \vec{A} :

$$\vec{A} = \frac{1}{\Delta} \begin{bmatrix} R_{sn} X_{rn} & k + \omega_{rn} X_{mn}^2 & -R_{rn} X_{mn} & \omega_{rn} X_{rn} X_{mn} \\ -k - \omega_{rn} X_{mn}^2 & R_{sn} X_{rn} & -\omega_{rn} X_{rn} X_{mn} & -R_{rn} X_{mn} \\ -R_{sn} X_{mn} & -\omega_{rn} X_{mn} X_{sn} & R_{rn} X_{sn} & k - \omega_{rn} X_{sn} \\ \omega_{rn} X_{mn} X_{sn} & -R_{sn} X_{mn} & -k + \omega_{rn} X_{rn} X_{sn} & R_{rn} X_{sn} \end{bmatrix}$$

where:

$$k = \omega_{cn} (X_{sn} X_{rn} - X_{mn}^2)$$

The electromechanical equation is:

$$T_{en} = \frac{T_e}{T_b} = 2 \left(\frac{1}{2} \frac{J \omega_b^2}{P_b (P/2)^2} \right) p_t \omega_{rn} + T_{ln} + B_n \omega_{rn}$$

where J is the moment of inertia, P_b is the base power, T_{ln} is the normalised load torque, B_n is the normalised friction coefficient of the load and motor and ω_{rn} is the normalised mechanical rotor speed, and

$$T_{en} = i_{qsn}^c \Psi_{dsn}^c - i_{dsn}^c \Psi_{qsn}$$

The modified flux linkages require additional computation. The torque can be conveniently expressed in terms of the normalised currents as:

$$T_{\text{en}} = X_{\text{mn}} \left(i_{\text{qsn}}^c i_{\text{drn}}^c - i_{\text{dsn}}^c i_{\text{qrn}}^c \right)$$

Solving these equations require numerical methods which are out of scope for this lecture. However, no one said one can't use SIMULINK which will be the topic of the next section.

2.5.1. Simulation Example

To get a better understanding of the equations derived previously, it is useful to do an example. To start let's define some parameters to use: We assume the motor stands at standstill. We apply a set of balanced three-phase voltages with a frequency of 50 Hz. The simulation diagram drawn in SIMULINK can be seen in **Fig. 2.9**.

As can be seen the initial model is relatively abstracted under sub-blocks. On the upper left part is the scopes of the variables which are of interest and on the upper-right is the variables which are to be saved to the work space. On the input block we define the other initial values for the simulation which are not defined in the .m file which are the step response torque load, three-phase voltage input, and the initial speed.

Before we start with the SIMULINK we need to initialise some variables which are as follows:

```

1  % Intialization
2
3  Rr      =1.15;           %Rotor resistance
4  Rs      =0.855;         %Stator resistance
5  Lls     =3.92e-3;       %Stator inductance
6  Llr     =3.92e-3;       %Rotor inductance
7  Lm      =30e-3;         %Magnetizing Inductance
8  fb      =50;            %Base frequency
9  p       =6;             %Number of poles
10 J       =0.06; %Moment of inertia
11
12 Lr       = Llr + Lm;
13 Tr       = Lr / Rr;
14 we       =2*pi*fb;
15
16 % Impedance and angular speed calculations

```

200 V	4 pole	3 phase	60 Hz
star connected	$R_s = 0.183 \ \Omega$	$R_r = 0.277 \ \Omega$	$L_m = 0.0538 \ \text{H}$
$L_s = 0.0553 \ \text{H}$	$L_r = 0.056 \ \text{H}$	$B = 0$	$T_l = 0 \ \text{Nm}$
$J = 0.0165 \ \text{kg m}^2$	$P = 4 \ \text{kW}$		

Table 2.1.: Simulation parameters for the IM example.

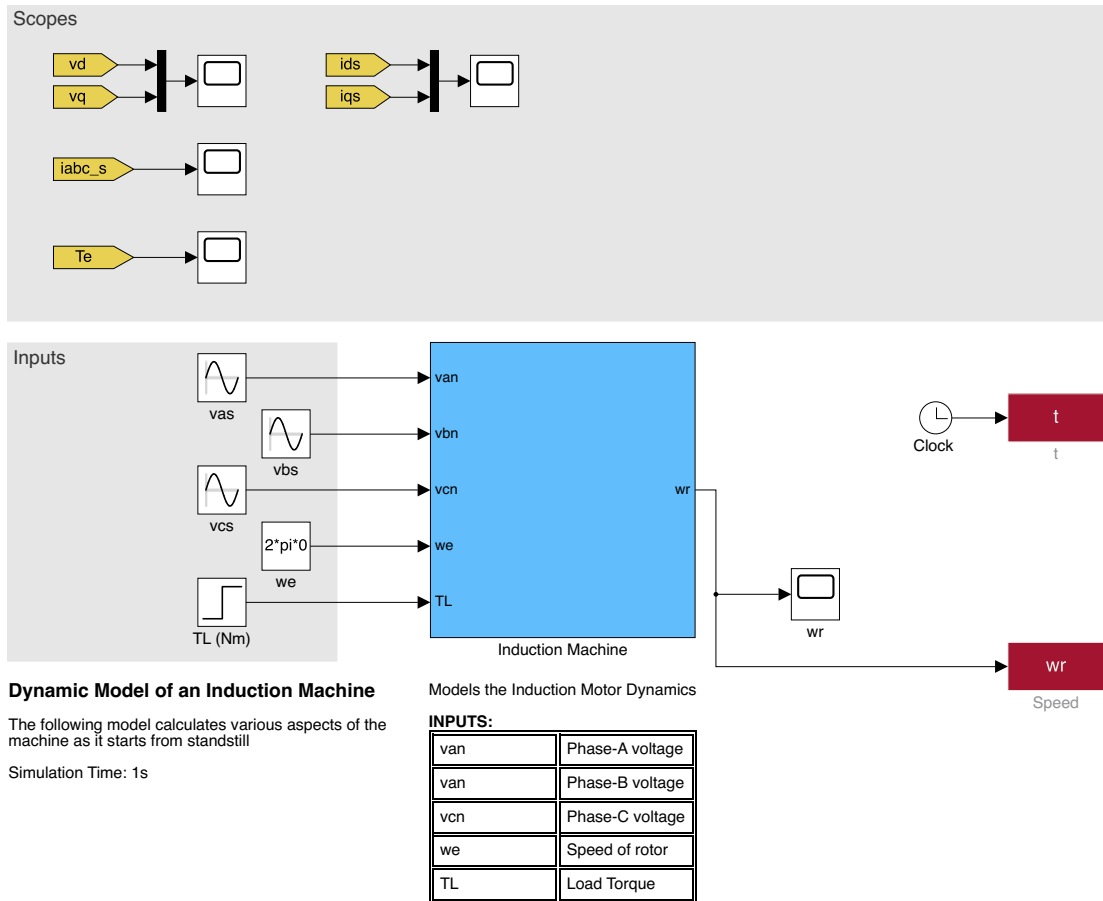


Figure 2.9.: A Simulink Model of an Induction Machine.

```

17
18 wb      =2*pi*fb;           %Base speed
19 Xls      =wb*Lls;           %Stator impedance
20 Xlr      =wb*Llr;           %Rotor impedance
21 Xm       =wb*Lm;           %Magnetizing impedance
22 Xmstar   =1/(1/Xls+1/Xm+1/Xlr);

```

C.R. 2
matlab

2.5.2. No-load Startup

We assume for this simulation the motor is not connected to any load but its own inertia. Before the simulation start, we should be aware, the rotor speed should be around %99-%98 of the synchronous speed. The results can be seen in **Fig. 2.12**.

Let's look at the figures from top to bottom. As can be seen the three-phase currents experiences a massive surge of current during its initial startup. This effect can be attributed to the inrush current experienced by any IM, where the inductive elements require a significant amount of current flow to generate the internal magnetic field to operate. Obviously, this can cause problem if **NOT**

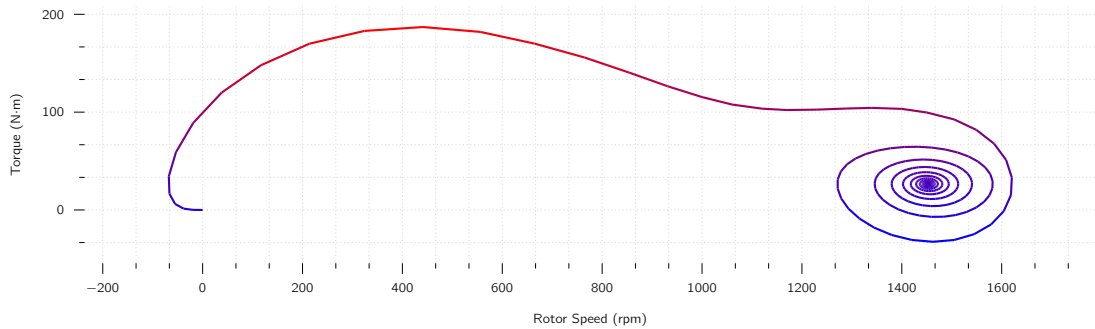


Figure 2.10.: The parametric plot of rotor speed v. torque when the motor starts from standstill without an external load.

taken care of as a massive surge of current during startup can cause the stator winding to melt and cause short circuit. There are methods to control this behaviour which was discussed in **B.Sc Drive Technology** course.

Next plot explains the torque development. As massive current surge happens, the motor experiences a significant torque production for a very brief time and as the rotor builds up speed the motor reaches a stable torque production.

The **dq0** transform allows us to remove the AC component of the signal and allows us to treat them as DC signal which we can easily observe.

The final plot to discuss is the i_d , i_q current which shows the effect of the induced current frequency. Observe in the beginning, the current has a relatively similar frequency value to that of the stator, but as the speed develops, the frequency dies down which is also observed.

The final aspect worth looking at is the **stability**. Of course if the motor does not produce stable torque at a given speed it's industrial relevance would be questionable. To that end let's observe it's speed v. torque given in **Fig. 2.10**. As can be seen there is only one (1) attractor and the system **converges** to that point without any oscillation or any orbit around a central point. This shows the stable behaviour of the motor.

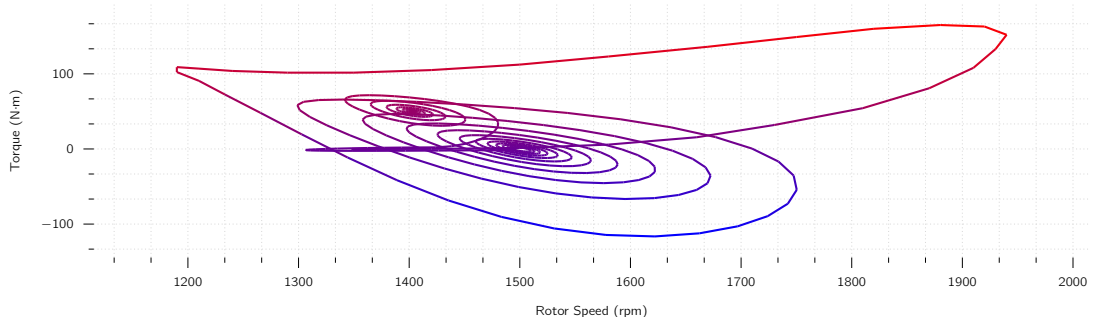


Figure 2.11.: The parametric plot of rotor speed v. torque when an instantaneous load is applied to the motor at 0.4 s.

2.5.3. Application of a Step Torque Load

It is of course normal for something to be **NOT** constant as the load experienced by the motor can change. This could be for situation such as the elevator, or any kind of transportation task where the load can change. This entails the study of these machines under different loads.

The previous simulation assumed a standard load connected to the shaft and the motor starts from standstill. Now, we will introduce a load of 50 N m to the shaft of the motor at the time s . Think of adding a shovel of cement to the cement mixer or dropping of items from a conveyor belt.

The simulation parameters are kept constant for both with only difference being the simulation time has been increased to 1 s to observe the transient effect. The simulation result are shown in X. As can be seen the 3-phase current experience a surge of current flow due to the increase of load the motor is required to handle and the stability is reached within 100 ms.

Looking at the **dq** current values of the it can be seen the sudden shift of the load increased the flow of i_{qs} while the i_{ds} current has just experiences an oscillation without a change in its amplitude. From here it can be seen the **torque-producing** part of the current is i_{qs} ³¹.

Final plot to look is the parametric plot in **Fig. 2.11**. As can be seen there are two (2) points of attraction. The first one on right is the initial stability point when the motor has no load whereas the second one on the left is the second point of stability. This plot tells us these **points of attraction** makes the machine operation stable and allow the safe operation under sudden load change.

³¹We will look into optimising this to control the machine performance, also known as **Vector Control**

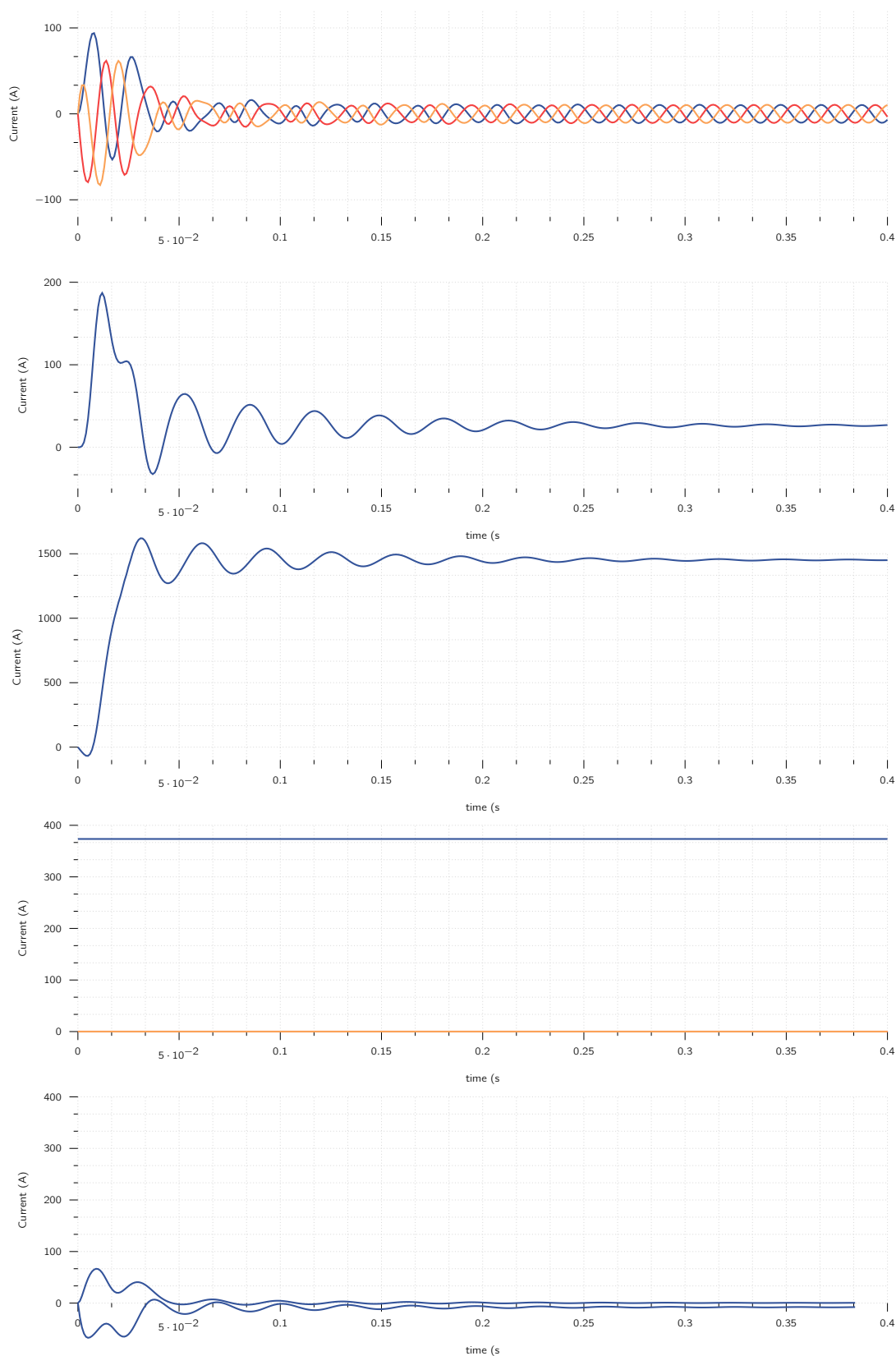


Figure 2.12.: Simulation results for starting IM from standstill.

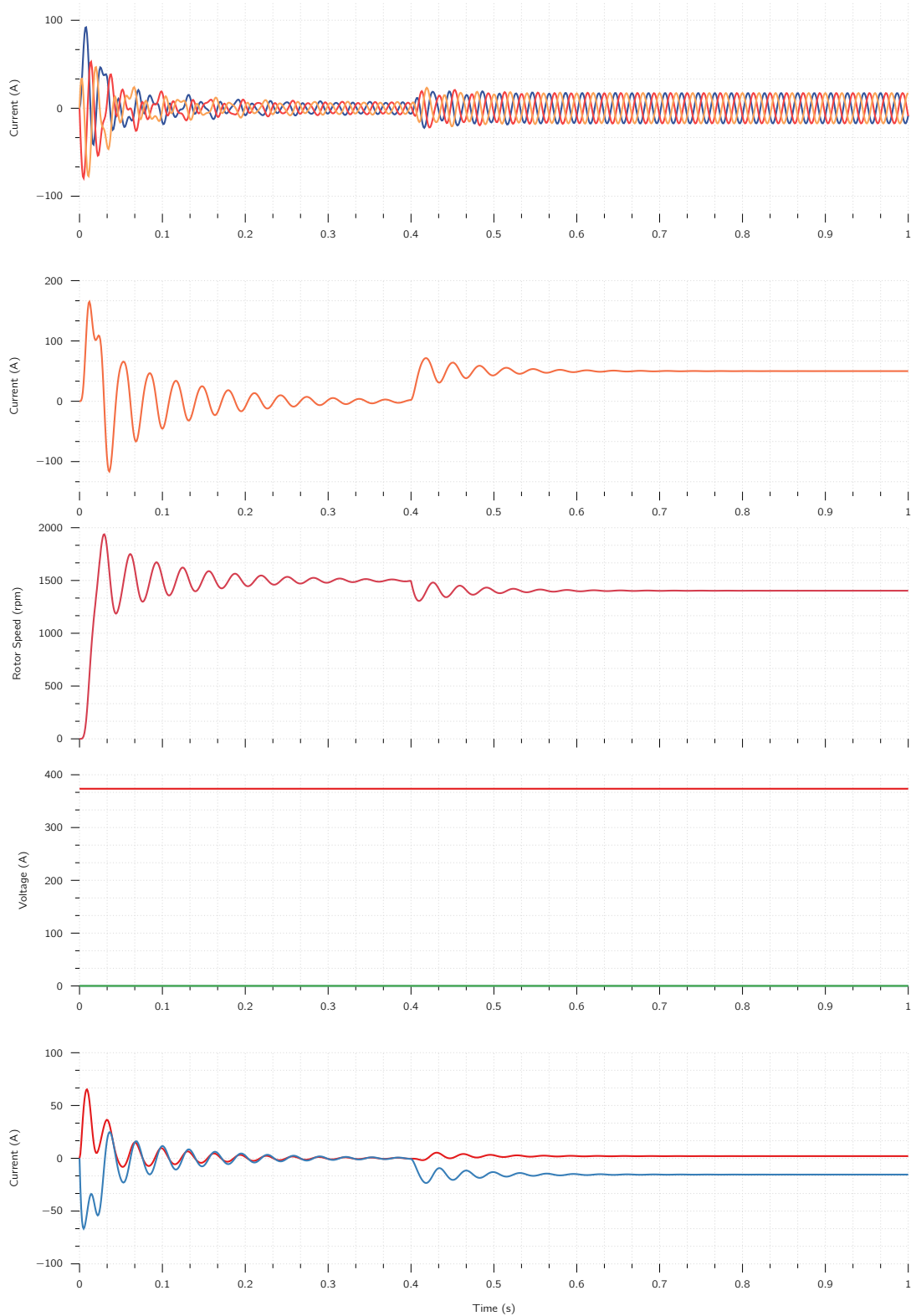


Figure 2.13.: Simulation of the IM when an instantaneous load is applied to the motor at 0.4 s.

Glossary

AC Alternating Current. 5, 9, 16, 18, 23, 24, 54

ANSI American National Standards Institution. 31

API American Petroleum Institute. 32

DC Direct Current. 1, 5–7, 9–18, 24, 42, 43, 48, 54

EMF Electro-motive Force. 5, 7, 10, 13–17, 28, 29, 43

IEC International Electrotechnical Commission. 31

IM Induction Machine. 1, 5, 6, 23–34, 39–41, 44, 46, 47, 49, 50, 52, 53, 56, 57

MMF Magneto-motive Force. 8, 34, 36, 39

NEMA National Electrical Manufacturers Association. 31, 32

PM Permanent Magnet. 5, 15

PMSM Permanent Magnet Synchronous Motor. 43

RHS Right Hand Side. 42

SCR Silicon Controlled Rectifier. 5

Bibliography

- [1] Ned Mohan, Tore M Undeland, and William P Robbins. *Power electronics: converters, applications, and design*. John wiley & sons, 2003.
- [2] M Nedeljković and Z Stojiljković. "Fast current control for thyristor rectifiers". In: *IEE Proceedings-Electric Power Applications* 150.6 (2003), pp. 636–638.
- [3] Galina Mirzaeva, Robert E Betz, and Terrence J Summers. "Evaluation of current density in DC motor brushes for mining machines based on air-gap field measurement". In: *IEEE Transactions on Industry Applications* 46.4 (2010), pp. 1255–1263.
- [4] Dimitris A Barkas et al. "Brushed DC motor drives for industrial and automobile applications with emphasis on control techniques: A comprehensive review". In: *Electronics* 9.6 (2020), p. 887.
- [5] Nuca Ilie et al. "Rehabilitation of the tram DC traction with modern power converters". In: *2014 International Conference and Exposition on Electrical and Power Engineering (EPE)*. IEEE. 2014, pp. 704–709.
- [6] David J Griffiths. *Introduction to electrodynamics*. Cambridge University Press, 2023.
- [7] Zurek. *Carbon brushes of small universal electric motor (circular saw)*. 2006. URL: https://commons.wikimedia.org/wiki/File:Carbon_brushes.jpg.
- [8] Electrical Academia. *DC Motor Assembly*. 2018. URL: <https://electricalacademia.com/wp-content/uploads/2018/03/DC-motor-field-structure-and-armature-assembly.jpg>.
- [9] H Wayne Beaty and Donald G Fink. *Standard handbook for electrical engineers*. McGraw-Hill New York, 2013.
- [10] Ernesto Soressi. "New life for old compound DC motors in industrial applications?" In: *2012 IEEE international conference on power electronics, drives and energy systems (PEDES)*. IEEE. 2012, pp. 1–6.
- [11] Dieter Gerling and Dieter Gerling. "DC-machines". In: *Electrical Machines: Mathematical Fundamentals of Machine Topologies* (2015), pp. 37–88.
- [12] Robert Stein et al. "Dc Motors". In: *Electric Power System Components: Transformers and Rotating Machines* (1979), pp. 398–442.
- [13] Polaris. *Motor Lamination*. 2025. URL: <https://www.polarislaserlaminations.com/motor-laminations.html>.

- [14] Arfat Siddique, GS Yadava, and Bhim Singh. "Applications of artificial intelligence techniques for induction machine stator fault diagnostics". In: *4th IEEE International Symposium on Diagnostics for Electric Machines, Power Electronics and Drives, 2003. SDEMPED 2003*. IEEE. 2003, pp. 29–34.
- [15] SI Malafeev and VI Konyashin. "Induction motor drives for electric mining shovels: synthesis, design and research". In: *2018 International conference on industrial engineering, applications and manufacturing (ICIEAM)*. IEEE. 2018, pp. 1–6.
- [16] Aveek Mangal. "Optimal control of induction machines under minimum energy in opencast mining machinery." In: *Journal of Mines, Metals & Fuels* 68.7 (2020).
- [17] Rajib Datta and VT Ranganathan. "Variable-speed wind power generation using doubly fed wound rotor induction machine-a comparison with alternative schemes". In: *IEEE transactions on Energy conversion* 17.3 (2002), pp. 414–421.
- [18] José Manuel Terras et al. "Estimation of the induction motor parameters of an electric vehicle". In: *2010 IEEE Vehicle Power and Propulsion Conference*. IEEE. 2010, pp. 1–6.
- [19] Derya Ahmet Kocabas, Emrah Salman, and Ahmet Kubilay Atalay. "Analysis using DQ transformation of a drive system including load and two identical induction motors". In: *2011 IEEE International Electric Machines & Drives Conference (IEMDC)*. IEEE. 2011, pp. 1575–1578.
- [20] indiamart. *Wound rotor induction motor*. 2025. URL: <https://www.indiamart.com/proddetail/wound-rotor-induction-motor-2851549755030.html>.
- [21] Hannu Karkkainen et al. "Converter-fed induction motor efficiency: Practical applicability of IEC methods". In: *IEEE Industrial Electronics Magazine* 11.2 (2017), pp. 45–57.
- [22] Juha Pyrhönen. "The high-speed induction motor: Calculating the effects of solid-rotor material on machine characteristics". In: *Acta Polytechnica Scandinavica, Electrical Engineering Series;(Finland)* 68 (1991).
- [23] Ion Boldea. *Induction Machines Handbook: Transients, Control Principles, Design and Testing*. CRC press, 2020.
- [24] Laurence HA Carr. "Recent progress in induction-motor construction". In: *Journal of the Institution of Electrical Engineers* 78.472 (1936), pp. 383–391.
- [25] Ali Challoop, Ahmed Sultan, and Mehdi Bonneya. "Improvement performance of squirrel cage induction motor using rotor bar skew". In: *AIP Conference Proceedings*. Vol. 2591. 1. AIP Publishing. 2023.
- [26] Chunyu Wang et al. "Analysis of vibration and noise for different skewed slot-type squirrel-cage induction motors". In: *IEEE Transactions on Magnetics* 53.11 (2017), pp. 1–6.
- [27] H Hafezi and A Jalilian. "Design and construction of induction motor thermal monitoring system". In: *Proceedings of the 41st International Universities Power Engineering Conference*. Vol. 2. IEEE. 2006, pp. 674–678.
- [28] Surajit Chattopadhyay, Aveek Chattopadhyaya, and Samarjit Sengupta. "Measurement of harmonic distortion and Skewness of stator current of induction motor at crawling in Clarke plane". In: *IET Science, Measurement & Technology* 8.6 (2014), pp. 528–536.

- [29] Subhasis Nandi, Shehab Ahmed, and Hamid A Toliyat. "Detection of rotor slot and other eccentricity related harmonics in a three phase induction motor with different rotor cages". In: *IEEE Transactions on Energy Conversion* 16.3 (2001), pp. 253–260.
- [30] Gene Collin Mechler. "Manufacturing and cost analysis for aluminum and copper die cast induction motors for GM's powertrain and R&D divisions". In: *Massachusetts Institute of Technology, Massachusetts* (2010).
- [31] *Rotating electrical machines - Part 1: Rating and performance*. Standard. Geneva, CH: International Electrotechnical Commission, 2007.
- [32] *Rotating electrical machines - Dimensions and output series - Part 1: Frame numbers 56 to 400 and flange numbers 55 to 1080*. Standard. Geneva, CH: International Electrotechnical Commission, 2007.
- [33] Jorma Luomi. "Transient phenomena in electrical machines". In: *Chalmers University, Sweden* (1998).
- [34] Akim Murakami and Sergey Edward Lyshevski. *Electromechanical systems, electric machines, and applied mechatronics*. CRC press, 2018.
- [35] Surajit Chattopadhyay et al. "Clarke and park transform". In: *Electric Power Quality* (2011), pp. 89–96.
- [36] He C Stanley. "An analysis of the induction machine". In: *Electrical Engineering* 57.12 (1938), pp. 751–757.
- [37] AM Wahl and LA Kilgore. "Transient starting torques in induction motors". In: *Transactions of the American Institute of Electrical Engineers* 59.11 (1940), pp. 603–607.

